

REVIEW

[View Article Online](#)
[View Journal](#) | [View Issue](#)Cite this: *Mater. Horiz.*, 2023,
10, 2824**Bioinspired humidity-responsive liquid crystalline materials: from adaptive soft actuators to visualized sensors and detectors**Ruochen Lan,^a Wenbo Shen,^b Wenhuan Yao,^c Jingyu Chen,^a Xinyu Chen^a
and Huai Yang^b

Inspired by nature, humidity-responsive materials and devices have attracted significant interest from scientists in multiple disciplines, ranging from chemistry, physics and materials science to biomimetics. Owing to their superiorities, including harmless stimulus and untethered control, humidity-driven materials have been widely investigated for application in soft robots, smart sensors and detectors, biomimetic devices and anticounterfeiting labels. Especially, humidity-responsive liquid crystalline materials are particularly appealing due to the combination of programmable and adaptive liquid crystal matrix and humidity-controllability, enabling the fabrication of advanced self-adaptive robots and visualized sensors. In this review, we summarize the recent progress in humidity-driven liquid crystalline materials. First, a brief introduction of liquid crystal materials, including liquid crystalline polymers, cholesteric liquid crystals, blue-phase liquid crystals and cholesteric cellulose nanocrystals is provided. Subsequently, the mechanisms of humidity-responsiveness are presented, followed by the diverse strategies for the fabrication of humidity-responsive liquid crystalline materials. The applications of humidity-driven devices will be presented ranging from soft actuators to visualized sensors and detectors. Finally, we provide an outlook on the development of humidity-driven liquid crystalline materials.

Received 15th March 2023,
Accepted 8th May 2023

DOI: 10.1039/d3mh00392b

rsc.li/materials-horizons**Wider impact**

Liquid crystalline materials are considered one of the most promising candidates as next-generation intelligent soft materials. Especially, humidity-responsive liquid crystal materials provide opportunities to manipulate these emerging functional materials in a harmless and instantaneous way. Thus, the design and fabrication of humidity-responsive liquid crystal systems have become a hot topic in the development of functional soft robots, advanced optical devices and biomimetics. However, there is no comprehensive review on this field. In this review, we provide a brief introduction on the humidity-responsive mechanism and liquid crystal materials. Subsequently, the strategies for the fabrication of humidity-responsive liquid crystalline materials are summarized and discussed. Based on the diverse functionalities of these materials, the applications of humidity-responsive liquid crystalline systems are introduced, including soft actuators, light manipulators, anti-counterfeiting devices and biomimetics. Finally, the outlook and challenges of humidity-responsive liquid crystals are presented. This review may provide inspiration for the design and preparation of soft intelligent materials and systems and give guidance for optimizing the complex responsivity of functional systems. Furthermore, it may attract interest from researchers related to biomimetic soft materials and hydrogels, liquid crystals, supramolecular chemistry and soft photonic crystals.

1. Introduction

Water is essential for life. In nature, water evaporates from liquid to gaseous state. This process plays a key role in the hydrologic cycle on Earth. In this case, humidity is used to represent the content of gaseous water in the atmosphere. Many plants perform biological functions according to the changes in humidity because humidity is a harmless and mild stimulation.^{1–6} Moreover, humidity changes readily occur in nature, and interact with plants in an isothermal way. For example, the morning glory

^a Institute of Advanced Materials & Key Lab of Fluorine and Silicon for Energy Materials and Chemistry of Ministry of Education, College of Chemistry and Chemical Engineering, Jiangxi Normal University, Nanchang 330022, China. E-mail: lanruochen@pku.edu.cn

^b School of Materials Science and Engineering, Peking University, Beijing 100871, China. E-mail: yanghuai@pku.edu.cn

^c Hangzhou WITLANCE Technology Co. Ltd, Hangzhou 310024, China

^d College of Chemistry and Chemical Engineering, Northwest Normal University, Lanzhou 730070, China

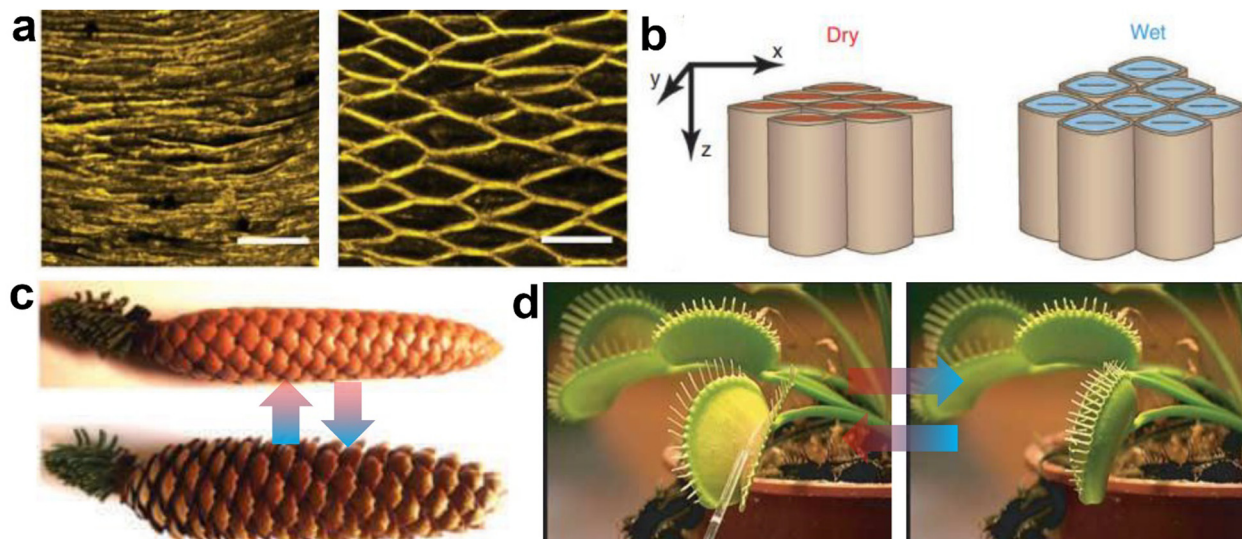


Fig. 1 (a) Lattice structure with hexagonal/elliptical-shaped cells in the dry (left) and wet (right) state. Scalebar: 0.1 mm. (b) Schematic illustration of hydration-dependent changes in shape. Reproduced with permission. Copyright 2011, Nature Publishing Group, a division of Macmillan Publishers Limited. (c) Humidity-responsive change shape of pine core, opening when dry (upper) and closing when rewetted (bottom). Reproduced with permission. Copyright 2009, Nature Publishing Group. (d) Venus flytrap in its open (left) and closed (right) states. Reproduced with permission. Copyright 2005, Macmillan Magazines Ltd.

flower blooms under high humidity and closes when the humidity decreases due to the high sensitivity of their petals to humidity changes. The mechanism of humidity-induced biological behaviors in plants can be mainly ascribed to the swelling and deswelling of their tissues under different humidity.⁷ As shown in Fig. 1a, the tissue cells of ice plants present a collapsed structure in the dry state. With an increase in humidity, cells are swollen by water. The deformation induced by the swelling of the cells is anisotropic, and thus the reversible humidity-induced shape changes in cells mainly occur along the Y direction, which is essential for the stable biological motions of plants (Fig. 1b). Based on this relatively simple principle, natural plants can perform various and complex motions.⁸ Pine cores have the ability to perform reversible humidity-responsive opening and closing, as shown in Fig. 1c.⁵ Their humidity-induced motion originates from

the motions of their surrounding tissues, which are composed of a fibre layer (8–12 μm) and sclereid layer (20–30 μm). Due to the large difference in the hygroscopic expansion coefficient between these two layers, slight changes in humidity can induce the macroscopic motion of the whole tissues.⁸ Another widely researched natural humidity-responsive behavior is the snapping of the Venus flytrap. In the normal state, the leaves of the Venus flytrap are open. However, when an insect approaches this plant, the induced humidity flow triggers the closing motion of its leaves (Fig. 1d). As one of the fastest movements in nature, the closure motion is within 100 ms due to the highly hydrated matrix of the leaf.¹

Taking lessons from nature, humidity-responsive artificial materials have been designed and developed by the fabrication of functional building blocks and construction of elaborated nanostructures, illustrating great potentials in various applications



Ruochen Lan

Ruochen Lan received his BS degree from the School of Materials Science and Engineering, Zhengzhou University in 2016. He received his PhD from the School of Materials Science and Engineering at PKU in 2021 and continued his research at PKU as a post-doctoral research fellow. His research interests focus on the synthesis of photo-responsive molecular machines, design of functional polymer materials, and fabrication of dynamic photonic crystals.



Huai Yang

Huai Yang is currently a professor at the School of Materials Science and Engineering, PKU. He received his PhD in engineering from Kyushu University in Japan, where he successively served as a visiting research fellow at the Faculty of Engineering. He was a research fellow at Fukuoka Industry, Science and Technology Foundation, as well as the Science and Technology Corporation in Japan (1996–2003). His research interests focus on liquid crystal/polymer composite materials, stimuli-responsive liquid crystalline polymers and smart windows.

ranging from soft actuators, sensors, and adaptive coatings to detectors and beyond.^{9–11} Among the stimuli-responsive materials, humidity-responsive materials possess superior advantages given that humidity changes are harmless, mild and instantaneous in the surrounding environment. Moreover, humidity-triggered responsiveness is an isothermal, untethered and silent process, suitable for reactions in both small volume and large space.^{12,13} To date, various humidity-responsive materials have shown distinct dynamic humidity-directed behaviors including graphene oxide (GO) materials, MXene composite materials, carbon nanotubes, metal–organic frameworks (MOFs), cellulose, polyionic liquids, azides, and polymers.^{14–19} Most efforts have been devoted to the preparation of humidity-driven actuators presenting various complex 3D motions such as bending, twisting and oscillating to convert humidity changes to mechanical output.^{17,20,21}

Liquid crystal (LC) materials are a class of emerging and appealing functional materials. In recent years, humidity-responsive LC materials such as LC polymers (LCPs), LC networks (LCNs) and cholesteric cellulose nanocrystals (CNCs) have been designed and prepared. Due to the programmable and anisotropic properties of LCs, humidity-responsive LC materials have been used in the fabrication of not only adaptive soft actuators but dynamic photonic crystals (PCs) with vivid color changes, serving as potential visualized sensors, coatings and detectors. Humidity-driven LC materials provide abundant opportunities for the development of advanced functional humidity-responsive materials and extend their potential applications in multiple fields. However, there is no comprehensive review on the recent development of humidity-driven LC materials. Accordingly, herein, this review provides a summary of the preparation, mechanism, potential applications and outlooks of humidity-responsive LC materials. Firstly, the properties of LC materials including LCs, LCPs, LCNs and CNCs, as well as guidelines for the preparation of humidity-responsive materials are introduced. Then, the strategies for the fabrication of humidity-driven LC materials are presented, which include the construction of inhomogeneous structures, bilayer and multi-layer strategy and modification of the material matrix. Finally, the applications of humidity-responsive LC materials as soft actuators, sensors, coatings and detectors are reviewed and the outlook of the development of this emerging class of materials is summarized. This review is expected to not only provide an introduction and the recent progress on humidity-responsive LC materials but deepen the understanding of the humidity-responsive mechanism and bring new twists in the design and fabrication of novel smart soft robots, advanced sensors and detectors and self-adaptive actuators.

2. General considerations

2.1 Liquid crystals

LCs are self-organized soft matter. In the LC phase, the molecules align anisotropically, combining the anisotropy of crystals and fluidity of liquids.²² The high mobility of LC molecules makes them sensitive to external stimuli, and thus they are

fascinating materials as a smart matter. In general, LCs can be classified into two categories, *i.e.*, thermotropic LCs and lyotropic LCs. The former represents materials showing the LC phase in a specific temperature range. Almost all thermotropic LCs are composed of organic molecules, exhibiting anisotropic shapes, such as rod shape, disc shape and banana shape. Lyotropic LCs refer to materials showing the LC phase when dissolved in a solvent with a certain concentration. Besides organic molecules or polymers, some inorganic materials such as graphene and metal oxide nanosheets can form an LC phase when dispersed in a solvent. According to the organization of the LC molecules, various types of LC phases are formed, such as nematic phase, smectic phase and cholesteric phase, as shown in Fig. 2a. In the smectic phase, the LC molecules self-assemble in layers, which is similar to that of solid crystals. However, the fluidity of LCs is poor in this case. LCs in the nematic phase are less ordered given that mesogens only present orientational ordering, as schematically illustrated in Fig. 2b. All the molecules align preferentially to one direction and the direction of molecular alignment is generally noted as the director (*n*). By adding a chiral dopant or grafting a chiral group on the mesogens, the cholesteric phase can be obtained, which is also named the chiral nematic phase (Fig. 2c). In this phase, the LC molecules gradually rotate along the direction perpendicular to the long axis of mesogens. The distance needed by cholesteric LC (CLC) molecules to rotate 360° is denoted as the helical pitch (*p*). CLCs are widely researched due to their ability to selectively reflect circularly polarized light (CPL) with a specific wavelength, acting as a one-dimensional PC. Due to their helical superstructure, the CLCs can divide iridescent light into two CPL with opposite handedness and reflect the CPL showing same the handedness as themselves, while transmitting another CPL (Fig. 2d). The reflection wavelength of CLCs is determined by *p* and the average refractive index (*n_a*) of the LC matrix, according to Bragg's Law as follows: $\lambda = p \times n_a$, where λ represents the reflection center. By adjusting the helical pitch, the photonic bandgap of CLCs can be precisely controlled, presenting an opportunity to prepare functional PCs with dynamic optical properties. In another

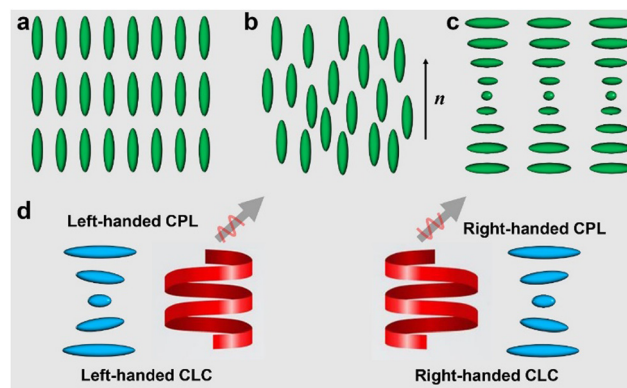


Fig. 2 Schematic illustration of mesogen alignment in (a) smectic phase, (b) nematic phase, and (c) cholesteric phase. (d) Demonstration of left-handed CLC and right-handed CLC and selective reflection of CLC materials.

intriguing phase, LC mesogens simultaneously twist along two directions, *i.e.*, helix direction and the direction perpendicular with the helix direction, which are named blue-phase LCs (BPLCs). This special LC phase occurs between the cholesteric phase and isotropic state. Rather than 1D PCs such as CLCs, BPLCs are a type of 3D PC showing a comparatively narrow reflection band due to their 3D periodic nanostructure.²³ As emerging functional 3D soft PCs, BPLCs can be prepared *via* the self-organization of building blocks without the requirement of external alignment. Moreover, laser emission can be realized in orthogonal three dimensions of BPLC materials, indicating the great potential of BPLCs for the fabrication of phase modulators, waveguiding lenses, *etc.*

2.2 Liquid crystal polymers and networks

Thermotropic small molar weight LCs are fluidic and only exhibit LC properties in a specific temperature range. Polymerizing reactive LC monomers in the LC phase can fix the ordered state of mesogens, resulting in freestanding and highly stable LCPs.^{24–26} Regarding the crosslinking density of LCPs, they can be classified as linear LCP (LLCPs), LC elastomers (LCES) and LCNs. LLCPs represent LCPs without any crosslinking points, which have a low melting point and poor mechanical property unless their molecular weight is high. LCES can be prepared by slightly crosslinking LCPs. They combine the liquid crystalline property, large deformation ability and resilience, presenting great potential for the fabrication of artificial muscles. When the crosslinking density is high, LCN materials can be obtained. These LC materials possess similar properties to that of thermoset polymers, showing high stiffness and tensile strength. Taking advantage of the integration of the anisotropy of LC and elasticity of polymers, LCPs can transfer molecular-scale disturbance into macroscopic shape changes with a programmable and adaptive way, enabling LCPs to be a powerful and intriguing matrix in the preparation of advanced smart actuators and devices.

Cholesteric LCPs (CLCPs) are prepared by “freezing” the helical superstructure of CLCs by polymer chains and networks, which endows them with selective reflection ability and superior mechanical performance. CLCP materials have attracted intense scientific interest due to their fascinating properties as light manipulators. For example, CLCP films that have a broad reflection band in the near-infrared region have been used as the cooling layer of buildings given that they decrease the incident near-infrared light in the daytime, lowering the temperature indoors. Simultaneously, they have no impact on the incidence of visible light, providing effective temperature regulation without energy consumption.²⁷ By finely tuning the photonic bandgap of CLCPs in the visible wavelength region, freestanding CLCP films showing vivid colors have been reported, illustrating potential for the preparation of chiroptical filters, photonic labels and anti-counterfeiting devices.^{28,29} In the case of CLC materials, the tunability of their photonic bandgap and superior mechanical property is contradictory. The helical pitch of small-molar-weight CLCs is totally dynamic. Both the length of the pitch and the handedness of the helix can be feasibly modulated due to the mobility of mesogens.

To obtain freestanding CLC films, the mesogens have to be polymerized or crosslinked, resulting in the loss of their chain mobility and pitch tunability. Although some thermochromic side-chain CLCPs have been reported, these materials were not crosslinked to ensure the self-adapting of mesogens, thus they had to be operated by coating on a matrix.^{30–32} Fortunately, this trade-off can be overcome by using water-swallowable CLCN materials. By endowing a CLCN film with hygroscopic property, the freestanding film could reversibly swell and shrink, resulting in changes in the pitch. In this case, the humidity-driven CLCN films possessing both superior mechanical performance and highly tunability of the helical pitch were prepared.³³

2.3 Cellulose nanocrystals

CNCs are needle-like nanorods with a length of around 1 μm and diameter of 10 nm. Considering that they are products from natural biomass, CNCs are renewable, abundant and biocompatible. As typical lyotropic LCs, CNCs can form a cholesteric phase when dispersed in a solvent with a specific concentration. The helical superstructure of CNCs can be retained by slowly evaporating the solvent, leading to the formation of a freestanding film showing structural colors.^{34–37} The intrinsic helical pitch of self-assembled CNC films is tunable by adjusting the size of the nanorods during the hydrolysis of the source. Due to the hydrophilicity of CNCs, self-assembled helical CNC films absorb water under high RH, enabling the swelling of the materials and elongating the helical pitch. When the RH is low, the material shrinks to its initial state due to water evaporation. The helical pitch also shortens during this process. The humidity-driven pitch changes endow CNC materials the ability to change their reflection colors, facilitating their application in the fabrication of humidity sensors and actuators.^{38–41}

More importantly, CNCs are a versatile matrix to load distinct responsive and functional elements.⁴² For example, to enhance the flexibility and mechanical strength of PC films, polymers or hydrogels can be integrated with CNCs. The resulting materials possess both the light-manipulating property of CNCs and superior mechanical property of polymers.^{43–45} The incorporation of thermo- or light-responsive parts with CNCs is an emerging strategy to fabricate dynamic chiroptical devices. In this case, the pitch or refractive index of the CNC matrix can be finely tuned by external stimulation.^{46–48}

2.4 Mechanism of humidity responsiveness

Humidity responsiveness in materials originates from the absorbing and desorbing of water. The mechanism of humidity-responsiveness is mainly based on several interactions between materials and water molecules, including hydrogen bonding, electrostatic interaction, and hydrophilic interaction.^{15,49,50} Swelling and shrinking of materials after combining with water or losing water provides most fundamental driving force of the humidity response. For instance, graphene oxide (GO) has abundant oxygen containing groups on its surface. In this case, the surface of GO absorbs water molecules by forming hydrogen bonds. Sun and coworkers reported the fabrication of a GO-based humidity-responsive actuator, in which one side had highly

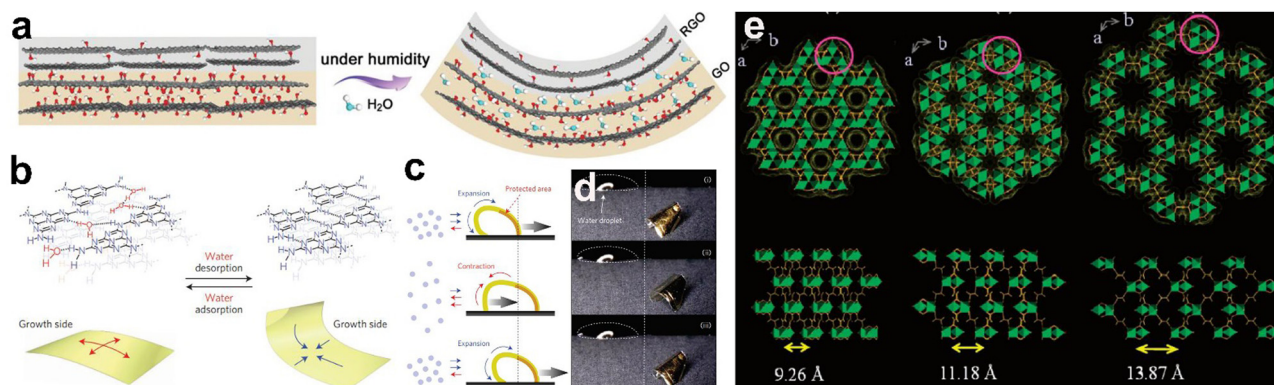


Fig. 3 (a) Schematic illustration of the humidity-driven bending behavior of the GO/RGO bilayer film. Reproduced with permission. Copyright 2015, Wiley-VCH Verlag GmbH & Co. KGaA, Weinheim. (b) Possible mechanism for humidity-responsive bending and folding behavior of carbon nitride film. (c) Schematic illustration and (d) real images of unidirectional walking of carbon nitride film. Reproduced with permission. Copyright 2016, Nature Publishing Group. (e) Simulated structures of the MIL-88 framework and its forms when swelling. Reproduced with permission. Copyright 2005, the American Chemical Society.

hydrophilic property.⁵¹ As illustrated in Fig. 3a, under high relative humidity (RH), the hydrophilic surface absorbed water, resulting in the swelling of this side. The inhomogeneous expansion made the GO film bend under high RH and recover when the RH decreased. The amplitude of swelling-induced deformation is partly dependent on the penetration depth of water. To drive large amplitude motions of macroscopic materials on the micrometer or centimeter scale, a relatively thick water-swellaible layer is required. However, in this case, the deformation rate is limited due to the slow water diffusion in the material bulk. To date, only when the film is ultra-thin, large amplitude and ultra-fast humidity-induced motions can be obtained. This is because the striking deformation of thin films can trigger ultra-fast swelling and shrinking of the film surface by a tiny amount of water.

For example, Aida's group reported the fabrication a humidity-sensitive ultra-thin carbon nitride film with a thickness of around 900 nm based on the hydrogen bonds between the nitride atom and water molecules, as shown in Fig. 3b.²¹ This material could perform autonomous motions in air due to the slight fluctuation in ambient humidity because the water molecules could only be absorbed by structurally defective sites rich in unreacted amino groups. Hence, the autonomous actuation could be driven by a minute amount of water. By protecting half of the film using a gold layer, a simple humidity-driven walker was prepared, as shown in Fig. 3c and d.

In contrast to ultra-thin inorganic materials, it is not possible to prepare large-scale and nanometer-thick LC films with considerable mechanical property and uniform alignment. Micrometer-scale water diffusion and swelling of material hosts provide the main driven force for humidity-responsive LC materials including LCP films and CNCs. Based on the fundamental principle, several strategies have been proposed to prepare humidity-driven LC materials, including water-induced LC order disruption by the hydrogen-bond of the material host and water molecules and water swelling of hygroscopic salty networks.⁵² These strategies will be introduced in detail in the following sections. Also, the construction of micro-pores in a polymer matrix with water-absorbing ability is an effective method.^{11,53}

Besides the swelling and shrinking of the whole matrix, embedding microscale humidity-sensitive parts in an inert material matrix is a versatile method to endow materials with humidity responsiveness.¹⁶ In 2005, Mellot-Draznieks and co-workers reported the synthesis of metal-organic-framework (MOF) materials showing reversible and large-amplitude humidity-driven volume changes by dynamically forming hydrogen bonds between absorbed water molecules and the inner groups of MOFs.⁵⁴ This process led to volume expansion of the MOF units (Fig. 3e). When exposed to a low RH atmosphere, the expanded MOF units shrunk to their initial state due to the loss of water. MasPOCH's group prepared a humidity-driven self-folding film by doping the MIL-88A MOF in polyvinylidene difluoride (PVDF). In their design, the composite film was prepared by mixing a polymer solution and MOF dispersion, followed by evaporating the solvent.⁵⁵ During this process, the MOF was deposited to the bottom side, resulting in an inhomogeneous distribution of MOF crystals along the thickness direction of the film. Under high RH, the bottom side of the film exhibited larger amplitude expansion than that of the top side, resulting in the bending and folding of the film. More recently, He and coworkers proposed another strategy to prepare humidity-driven MOF/polymer composite films with high sensitivity by uniformly dispersing MOF crystals in a polymer matrix with gradient crosslinking density.⁵⁶ Humidity-driven LC materials could also be prepared by integrating a humidity-responsive part in an ordered LC host. Interpenetrating hygroscopic networks with anisotropic LCP networks have been proved to be effective for the fabrication of water-sensitive LC materials, which is the preferred method to fabricate humidity-driven LC devices with enhanced performances in some cases.⁵⁷ For example, a water-swellaible CLCN coating prepared by interpenetrating hygroscopic networks in a CLCN host presented wider reflection band tuning range compared with that of the pure activated CLCN host.^{33,58,59}

The mechanism of humidity-responsive materials is not complicated, and consequently with the synthesis of new materials, the development of advanced processing techniques and construction of novel micro-nano structures, various humidity-responsive

materials including organic, inorganic and composite materials showing diverse and complex functionalities have been reported, paving the way to fabricate novel smart materials with high sensitivity and adaptivity to the surrounding environment.

3. Strategies for the fabrication of humidity-responsive LC materials

Humidity-driven LC materials can be mainly classified into shape-changeable actuators including LCNs and LCEs, color-changeable PCs such as CLCNs and CNCs and structural color actuators, integrating both shape changing and color changing abilities. However, it is necessary to develop advanced fabrication techniques and ingenious strategies to realize multifunctional humidity-driven LC actuators and PCs with complex and on-demanded motions and light modulation abilities. Generally, homogeneously structured LC materials respond to humidity or water by performing in-plane contraction and expansion, while inhomogeneous-structured LC materials perform out-of-plane movements when subjected to humidity triggers.⁶⁰ According to the structure of materials, all humidity-responsive LC materials can be classified into homogeneous structures and inhomogeneous structures; however, this classification is broad and not precise. In this section, we introduce the strategies for the fabrication of humidity-driven LC materials by discussing the most representative preparation methods. The mechanism of each strategy and performance of materials prepared by different fabrication methods will be provided.

3.1 Construction of inhomogeneous structure

In materials design, asymmetric local deformation can drive complex 3D shape changes of the whole material. Materials with an inhomogeneous structure perform out-of-plane and designable motions under a uniform stimulation field due to the distinct responsiveness between different domains. In the case of LCP materials, constructing gradually changed molecular alignment across the film thickness provides symmetry-breaking force and drives the complex out-of-plane movement of the LCP films (Fig. 4a).^{61–64} Broer's group realized a humidity-responsive LCN film showing reversible bending and curling motions *via* the construction an alignment gradient along the thickness of the film.⁶⁵ Due to the difference in molecular alignment, the swelling behavior of the two sides was different. In a homogeneous humidity air environment, the twist aligned film bent rapidly due to the synergistic deformation of the two sides (Fig. 4b). By post-treating the uniform LCN film, an inhomogeneous structure presenting a gradient in hygroscopic property could be achieved.

The second strategy to construct an inhomogeneous structure is based on imbalance chemical treatment. Schenning *et al.* prepared a hydrogen-bonded LCN film using carboxylic acid, as presented in Fig. 4c. By soaking one side of the film with KOH solution, the hydrogen bonds broke due to the conversion of carboxylic acid to carboxylic salt.⁶⁶ The resulting film adopted a bending shape because of the collapse of the treated side. Under high RH, the hygroscopic side absorbed water and swelled, while the other side

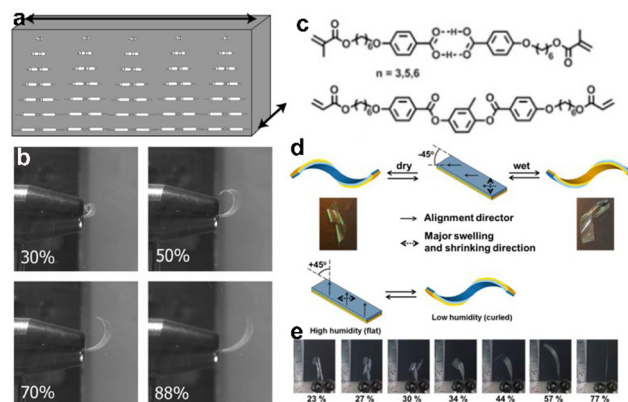


Fig. 4 (a) Illustration of mesogen alignment in twist-aligned LCN film. (b) Humidity-responsive shape changes in twisted LCN film under different RH. Reproduced with permission. Copyright 2005, the American Chemical Society. (c) Chemical structures of LC monomers used in ref. 65 and 66. (d) Schematic illustration and (e) real images of humidity-induced motions of film with the molecular director at a 45° angle with respect to the long axis of the film. Reproduced with permission. Copyright 2014, the American Chemical Society.

was unchanged, causing a change in bent to unbent shape. When the RH decreased to the initial state, the reverse shape change occurred. Due to the highly tunable mesogen alignment in the LCN matrix, different humidity-driven motions including curling and twisting were programmed (Fig. 4d and e). This method relies on the breakage of the hydrogen bonds and collapse of the ordered LC structure, making the prepared LCN film present curling or bending shape in a normal atmosphere. Recently, Kim and coworkers reported a new class of dimethylamino-functionalized humidity-driven LCE films (Fig. 5a and b). The film could be activated using acidic solution due to the formation of ionic groups on the treated side, as schematically illustrated in Fig. 5c.⁶⁷ The ionized side of the film became hygroscopic (Fig. 5d). By increasing the RH, the acidified side absorbed water and expanded, while the other side was hydrophobic, resulting in the directional bending of the whole film. By activating specific regions of one side of the film, arbitrary shapes of the LCE film were achievable by increasing the RH due to the reversible humidity-driven swelling of the hydrophilic regions (Fig. 5e).

Typically, the amplitude of the shape change of LCN materials is hindered by their crosslinking density. Accordingly, Katsonis's group prepared a humidity-driven LCN film with large amplitude deformation by construct a crosslinking density gradient in the LCN film.⁶⁸ By activating the film using a base solution, the loosely crosslinked side of the film underwent larger amplitude swelling compared with that of densely crosslinked side when exposed to high RH. This phenomenon led the film undergoing reversible humidity-driven shape transformation. By further controlling the molecular alignment, diverse humidity-responsive actuation modes of the LCN film were realizable.

3.2 Bilayer strategy

Although inhomogeneous humidity-responsive LC materials can perform complex deformations under uniform RH changes, they

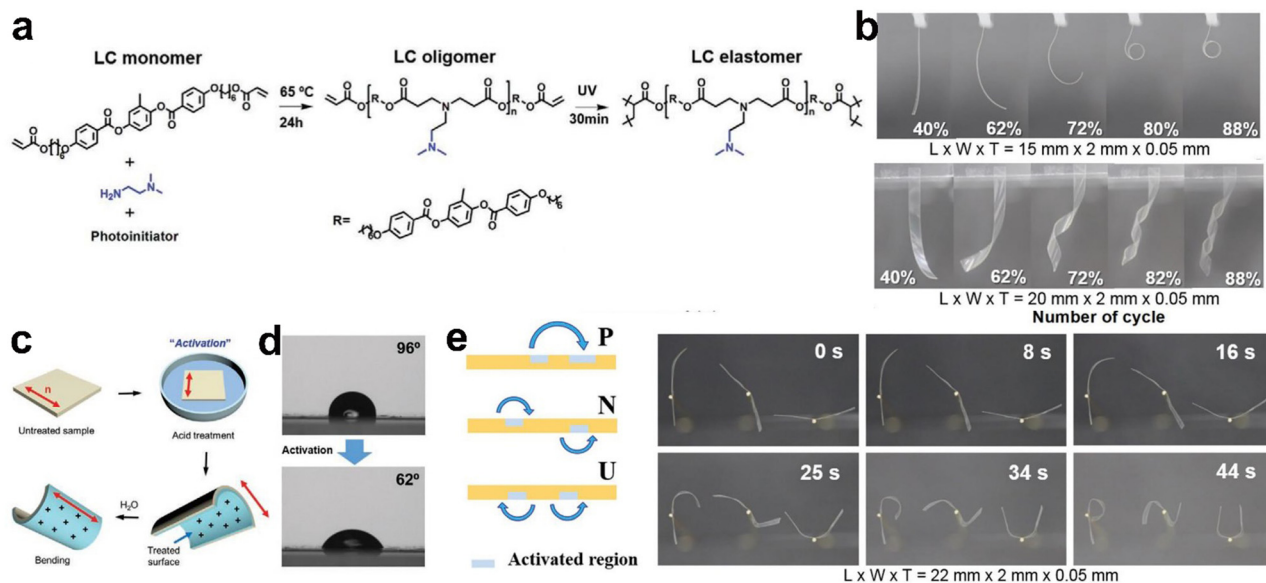


Fig. 5 (a) Chemical structure and polymerization process of LCE by aza-Michael addition reaction. (b) Bending (upper) and twisting (bottom) of LCE film under different RH. (c) Schematic illustration of activation by acidic solution. (d) Contact angles of the LCE surface before and after activation. (e) Illustration of activated regions in three LCE films to obtain the shapes of letters "P," "N," and "U," and the process of these three films transforming into the desired shapes with increasing RH. Reproduced with permission. Copyright 2021, Wiley-VCH GmbH.

suffer from several limitations including tedious fabrication and moderate sensitivity. Fabricating highly sensitive humidity-driven devices *via* a facile process employing the bilayer strategy has distinct advantages such as programmability and superior compatibility.⁶⁹ Bastiaansen *et al.* proposed the fabrication of a humidity-driven bilayer actuator by coating a hydrogen-bonded LCP layer on an oriented polyimide-6 (PA-6) substrate (Fig. 6a).⁷⁰ The prepared composite film presented a bending shape due to its shrinkage after polymerization. After breaking its hydrogen bonds, the film adopted a more bent shape due to the collapse of the LC structure. With an increase in the RH, the LCP side absorbed water and expanded, driving the whole film deformation from bending shape to flat shape because of the joint effects of water-swelling of the LCP layer and higher expansion coefficient of the splay-aligned LCP layer compared with that of the PA-6 layer, as illustrated in Fig. 6b. One of the merits of the bilayer strategy is its high programmability, Schenning and coworkers proposed a highly programmable bilayer humidity-responsive LCP actuator by spray-coating a chiral nematic LCP film on a hydrophilic PA-6 substrate.⁷¹ In this case, the activation of LCP by a base solution was not required because the helically organized LCP layer only tuned the mechanical anisotropy. By changing the RH, the hydrophilic PA-6 substrate absorbed or desorbed water, providing actuating force for deformation. More importantly, the deformation modes of the bilayer film were adjusted by changing the twisting angle of the LC mesogens across the thickness of the LCP film. As presented in Fig. 6c, the prepared humidity-driven bilayer actuator presented high programmability, where not only the types of motions such as bending and twisting but the twisting pitch of the film could be tuned by changing the twisting angle of the mesogens. Due to the superior compatibility provided by the bilayer strategy, our group prepared a humidity-responsive

composite film showing synergistic shape and fluorescence changes.⁷² The hydrogel layer of the hybrid film was hygroscopic and could swell or shrink with a change in the RH, actuating the humidity-responsive motions of the bilayer film. Simultaneously, the hydrogel film acted as a loading matrix for functional fluorescence molecules, avoiding the disturbing effect when doped in the LCN matrix.

Water-responsive CNC materials have a uniform helical structure, and thus perform out-of-plane deformation only when one side is swollen by water.⁷³ In this case, the construction of a bilayer structure using a CNC layer as the active layer has been proven to be effective to realize programmable and large amplitude motions of films under uniform RH changes.⁷⁴ Zhang's group reported that a CNC-based bilayer film exhibited synergistic humidity-driven motions and structural color changes.⁷⁵ By incorporating a polyurethane (PU) layer in a CNC layer, the hybrid film performed humidity-driven motions due to the swelling ability of the CNC layer. Besides, the low thermal expansion coefficient of the CNC layer enabled the film to undergo near-infrared light driven bending by thermal expansion mismatch of the two layers (Fig. 6d). Moreover, the helically aligned CNC film endowed the bilayer film vivid structural color and obvious color changes during its actuation process, illustrating the potential of this novel CNC film in the anti-counterfeiting and information storage fields, as shown in Fig. 6f.

3.3 Interpenetrated networks

Interpenetrating polymer networks (IPN) represent two interwoven polymer networks without covalent bonding between them, which is a straightforward method to combine the functionalities of multiple components into a single material system.

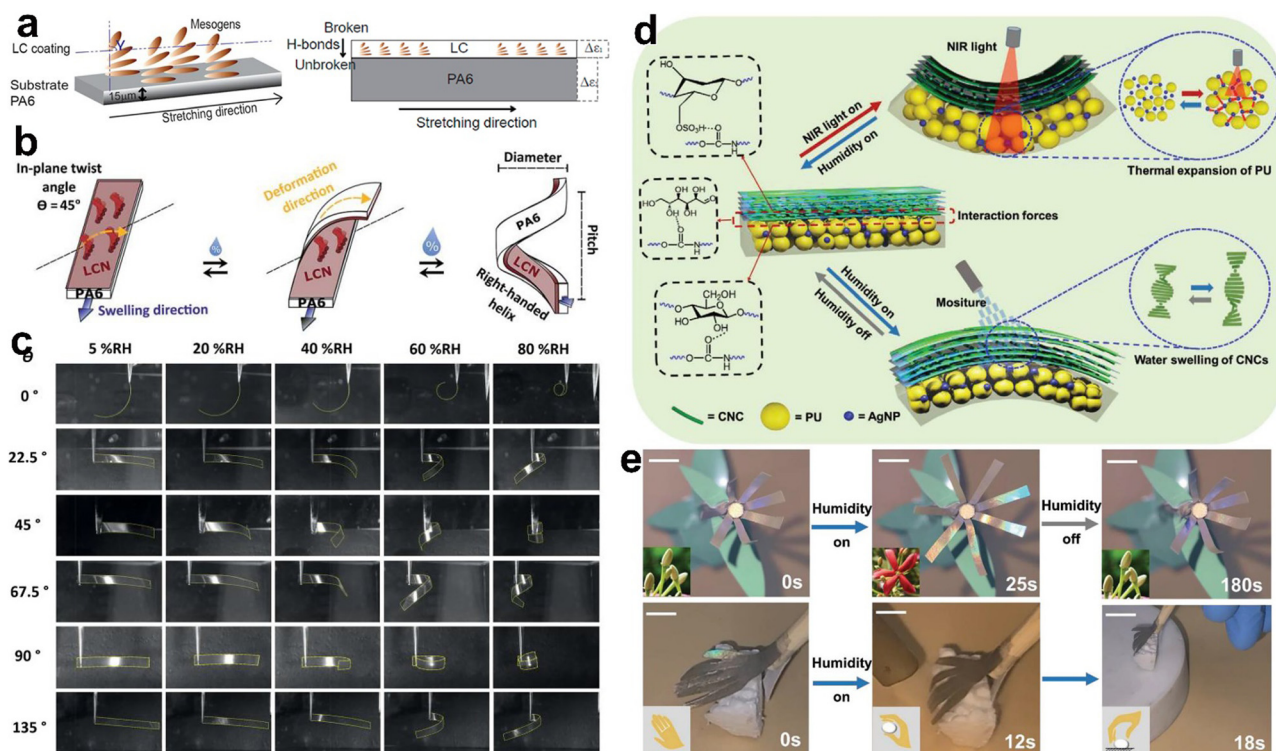


Fig. 6 Schematic illustration of (a) splay-aligned LCN coating and (b) twist-aligned LCN coating on the PA-6 substrate. Reproduced with permission. Copyright 2013, the American Chemical Society. (c) Shape changes of bilayer actuators in response to RH changes. Reproduced with permission. Copyright 2018, The Royal Society of Chemistry. (d) Illustration of the bilayer composite film based on CNCs and inverse opal structure and its NIR light- and humidity-responsive principles. In the chart, PU means polyurethane. (e) Applications of the humidity-driven bilayer actuator: a smart "Rangoon creeper flower" and a "palm" grasp and transfer an object to the destination. Scale bars, 1 cm.

LCP-based IPNs are attractive and intriguing because they can endow intrinsic anisotropy to diverse polymer matrices.^{76–79} IPNs are homogeneous structures, which are not advantageous in the preparation of actuators with complex deformation modes. Thus, the IPN strategy is often used in realizing color-changing CLC materials. Stumpel and coworkers interpenetrated a water-swellaible poly(acrylic acid) hydrogel in a CLCN film, realizing dynamic reflection bands of the composite film stimulated by pH and humidity.⁵⁷ The reversible swelling and deswelling hydrogel network triggered the elongation and shrinkage of the helical pitch of the helically organized CLCN layer (Fig. 7a). By introducing a non-swellaible network in specific regions, water-responsive colorful patterns could be constructed, as shown in Fig. 7b. The water and pH-responsive structural color changes of the CLCN layer were coincident with the changes in the thickness of the film, as presented in Fig. 7c and d. To improve the stability of humidity-responsive LCP-based IPN materials, de Haan and coworkers used poly ionic liquids as components and prepared humidity-driven CLCN coatings, showing wide band-shifting range and high stability without the requirement of base activation.⁸⁰ In the preparation process, the small-molar-weight LC 5CB was used to occupy volume during the polymerization process. After the removal of 5CB in polymerized film, the ionic liquid could fill it, making it possible to regulate the water response of the IPN film by changing the content of 5CB (Fig. 7e). Accordingly, the humidity-driven CLCN

coating prepared using this method presented a stable water response and no fatigue after one month usage (Fig. 7f). The IPN strategy provides opportunities to functionalize humidity-driven LCP systems.⁸¹ For example, a humidity-responsive poly(acrylic acid) and CLCN interpenetrating network enabled the fabrication of visualized biosensors due to the interaction between acrylic acid and various species including urea, glucose, biotin and uric acid.⁸² As schematically illustrated in Fig. 7g, the mechanism of the biosensor relied on the internal pH changes due to bioreactions, leading to the swelling or deswelling of the CLCN matrix. Due to the visible color changing behavior, this biosensor was versatile in detecting various biochemicals and their concentration (Fig. 7h and i).

4. Applications of humidity-responsive LC materials

4.1 Soft actuators

Humidity changes provide signals and driving force for some biological behaviors of natural plants, such as the blooming and closing of flowers. Advanced artificial materials that can convert humidity changes to mechanical output are appealing in the development of next-generation intelligent systems. As emerging humidity-driven soft actuators, LC-based materials possess programmable property and mechanical anisotropy,

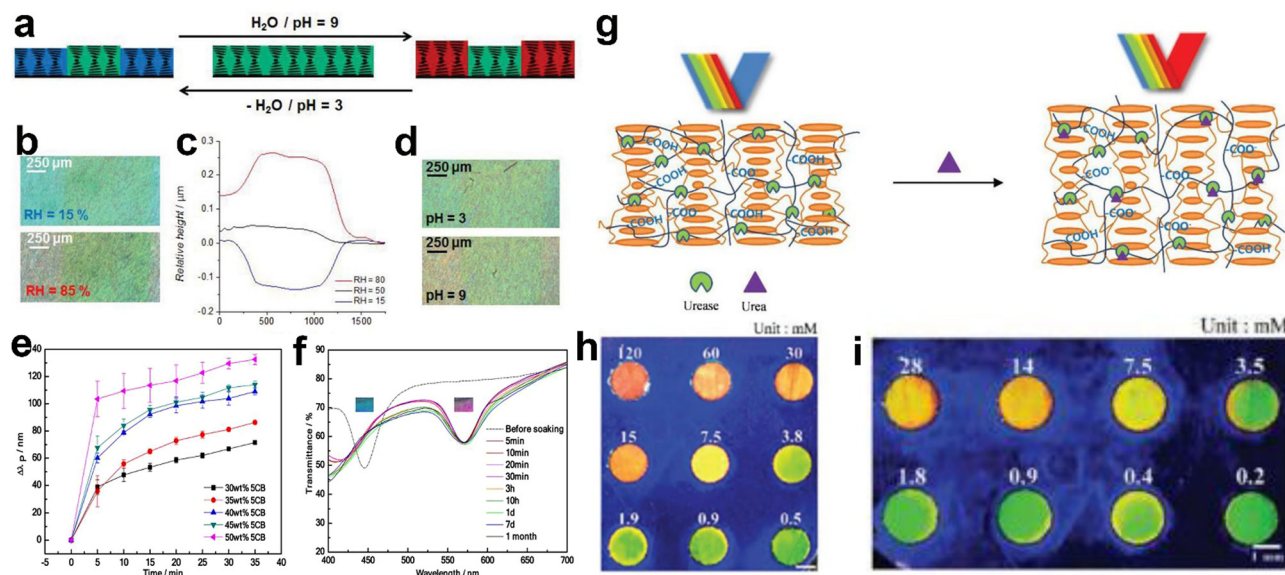


Fig. 7 (a) Schematic of the mechanism of the poly(acrylic acid)-CLCN IPN. (b) Optical micrographs of a patterned IPN coating at RH of 15% and 85%. (c) Surface topography of the patterned humidity-responsive IPN coating at RH = 15%, 50%, and 80% at room temperature. (d) Optical micrographs of the patterned IPN polymer film at pH of 3 and 9. Reproduced with permission. Copyright 2015, Wiley-VCH Verlag GmbH & Co. KGaA, Weinheim. (e) Humidity-responsive band shift of IPN coating of poly(ampholyte) and CLCN based on various amounts of 5CB. (f) Stability test of IPN coating of poly(ampholyte) and CLCN with 50 wt% of 5CB. The inset images show the colors of coating in the wet and dry states, respectively. Reproduced with permission. Copyright 2019, the American Chemical Society. (g) Schematic of the sensing mechanism of the CLC-hydrogel-IPN biosensor. Images of CLC-hydrogel biosensor (h) when interacting with different concentrations of urea and (i) after dropping human serum buffer solution with different concentrations of urea. Reproduced with permission. Copyright 2018, Wiley-VCH Verlag GmbH & Co. KGaA, Weinheim.

enabling the on-demand design of functional actuators with complex motions and self-adaptivity. The use of humidity as a trigger to motivate motions in LC-based soft actuators generally involves two approaches.

One is wetting only one side of the material. For example, Yu's group found that an azobenzene-crosslinked LCN film performed unidirectional motions when one side of the film was treated by moisture.⁵² The humidity-driven deformation always occurred along the direction perpendicular to the molecular director because of the joint effect of water swelling and loss of molecular order due to the hydrogen bonds between the water molecules and C–O–C groups. Exposing the film to UV light excited the isomerization of azobenzene, leaving the film bending along the aligned direction, as demonstrated in Fig. 8a. The orthogonal humidity and photo dual responsiveness facilitated the preparation of a multifunctional soft switch to control the on-off of two light-emitting diode (LED) lights. As shown in Fig. 8b, two electrical circuits responsible for yellow LED and red LED were controlled by the LCN film. Exerting moisture to one side of the film or illuminating the film by UV light could turn on the yellow LED and red LED, respectively, illustrating the potential of this humidity-driven LCN film in touchless electronic devices.

Helically structured cholesteric CNC materials are intrinsically humidity responsive, providing opportunities to fabricate adaptive soft actuators showing vivid structural colors. Guo's group sandwiched a stretching-aligned PA6 film by two CNC layers, realizing reversible and programmable humidity-directed motions of the structural colored film (Fig. 8c).⁸³

Although the chirality of both of CNC layers were left-handed, the composite film presented hyper-reflection at a specific wavelength due to the half-wave retardation effect provided by the inner PA6 layer. By modulating the alignment of the PA6 layer by changing the cutting direction, bending and twisting motions could be observed by treating one side of the actuator using moisture, as shown in Fig. 8d. Another type of humidity-driven soft actuators can be motivated by changing the environmental RH, which is regarded as a more convenient and efficient approach. Since the method to prepare humidity-responsive LCN actuators by alkalizing one side of the hydrogen-bonded LCN film was put proposed in 2014, several works have been done to extend the applications and functionality of novel LCN actuators.⁶⁶ Integrating photothermal dyes in the LCN matrix can build interplays between light-heating and humidity-responsiveness. A humidity-driven LCN actuator was obtained by alkalizing the homotropic side of a hydrogen-bonded splay-aligned LCN film.⁶⁴ The actuator changed between bending shape and less bending shape due to the expansion of the homotropic side of the film under different RH. Moreover, due to the doped photothermal dyes, the film became inert to the humidity when exposed to light because water evaporated from the film rather swelling the matrix, as illustrated in Fig. 8e. Using the dual-responsive LCN actuators, a humidity-responsive nocturnal flower that only bloomed in the dark was achieved, as illustrated in Fig. 8f.

Besides their adaptivity to different triggering methods, humidity-driven LC-based soft actuators can also be feasibly functionalized to realize complex and on-demanded motions.

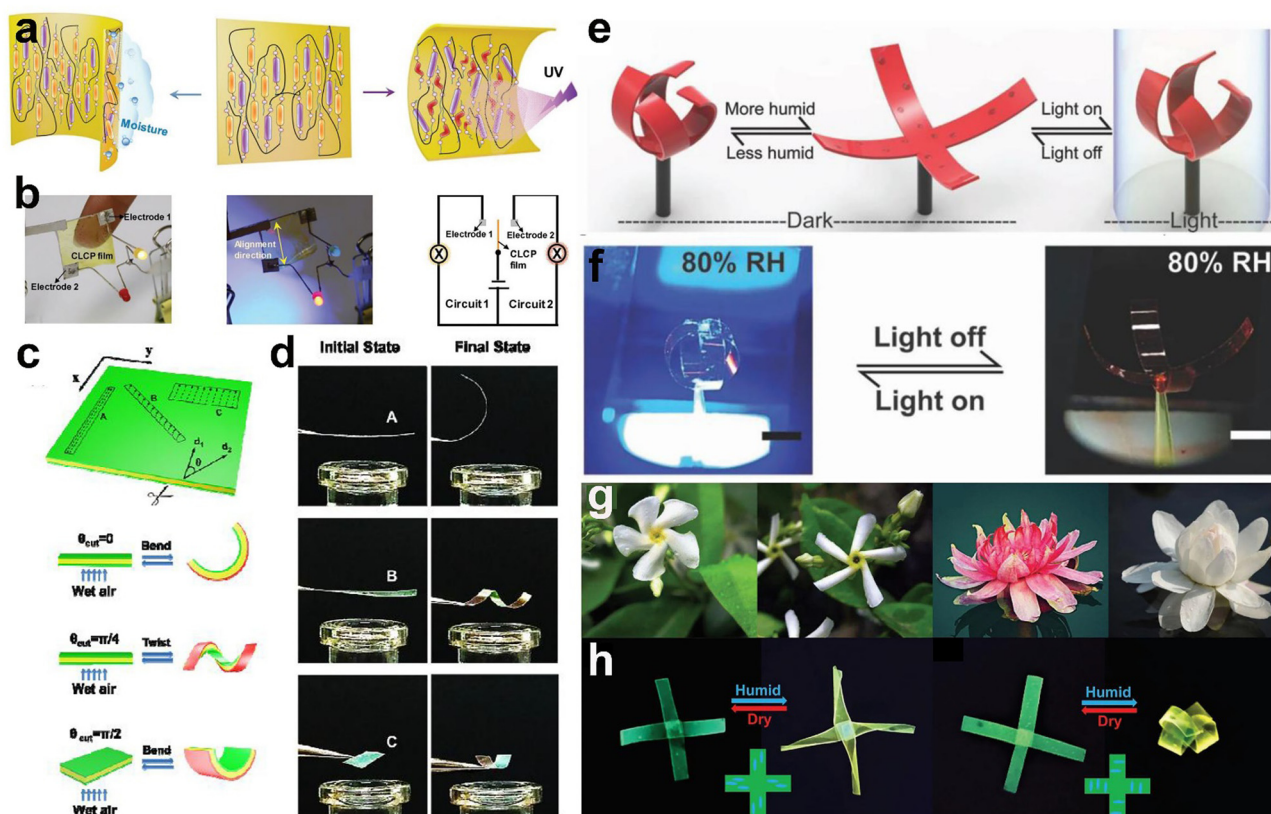


Fig. 8 (a) Schematic representation of the humidity- and photo-responsive deformation principle of azobenzene-crosslinked LCN films. (b) Dual-mode actuator that controls two LED lights of different colors and its working mechanism. Reproduced with permission. Copyright 2017, Wiley-VCH Verlag GmbH & Co. KGaA, Weinheim. (c) Illustrations of various actuation modes of a sandwich film of CNCs and oriented PA-6. Reproduced with permission. Copyright 2016, The Royal Society of Chemistry. (d) Humidity-driven bending and twisting deformation of sandwich film of CNCs and oriented PA-6. Reproduced with permission. Copyright 2016, The Royal Society of Chemistry. (e) Schematic illustration and (f) real images of stimuli-responsive blooming and closing of humidity and light-dual responsive artificial nocturnal flower. Reproduced with permission. Copyright 2018, Wiley-VCH Verlag GmbH & Co. KGaA, Weinheim. (g) Blooming and closing of natural Confederate Jasmine and petals. (h) Artificial fluorescent flower that imitates Confederate Jasmine and petals. Reproduced with permission. Copyright 2021, Wiley-VCH GmbH.

Our group realized the first example of a humidity-driven LCN actuator showing synergistic fluorescence changes by incorporating a hydrophilic hydrogel layer and hydrochromic aggregation-induced emission (AIE) luminogens in an LCN matrix.⁷² With changes in RH, the hydrophilic layer contracted or expanded, actuating the deformation of the composite film. Meanwhile, the fluorescence color reversibly changed simultaneously due to the interaction of the AIEgens with water molecules. The mechanical anisotropy provided by the LCN layer converted the simple contraction and expansion of the hydrogel layer into complex and programmable motions of the film. As shown in Fig. 8g and h, the programmable humidity-responsive LCN actuator showing synergistic fluorescence color change has potential to mimic complex biological motions, such as synergistic blooming and color changing of Confederate Jasmine and petals. More recently, a novel reprogrammable humidity-driven LCN actuator was prepared by introducing ionic crosslinks in an ordered LCN matrix.⁸⁴ The hygroscopic carboxylic salty network could be locked by ions, losing its water absorbing ability. In this case, the water swellable regions could be arbitrarily controlled, resulting in diverse and programmable deformation of the LCN film with a change in RH.

More importantly, the ionic crosslinks are physical bonds that can break by other treatments, enabling the reversible modification of the LCN film and reprogrammable humidity-driven motions.

The performance of humidity-driven soft actuators is also related to their fabrication process. CNC materials with a periodic helical structure can be formed *via* evaporation-induced self-assembly (EISA). By controlling the concentration of CNC nanorods in solution, the helical pitch of the obtained CNC film could be finely tuned. MacLachlan's group prepared a humidity-responsive bilayer structural colored film using a CNC layer as the template.³⁸ As illustrated in Fig. 9a, the reflection bands of the two layers could be individually modulated by changing the concentration of the CNC nanorods or doping salts in the precursor solution. Consequently, a colorful film showing humidity-directed 3D motions was obtained due to the mismatch in the expansion between the two layers (Fig. 9b). At a suitable concentration, the CNC nanorods aligned directionally to form a nematic phase. By depositing the nematic CNC layer on a soft and porous substrate with different water swelling ability, Zhu and coworkers reported a humidity-driven actuator with high response speed and high sensitivity. It was found that

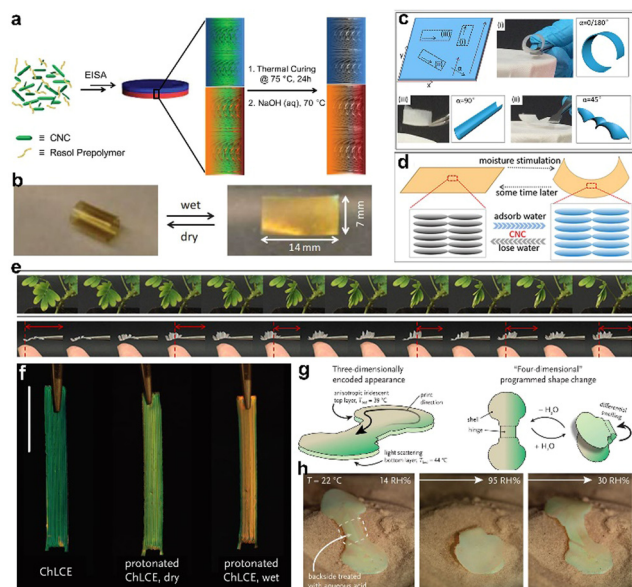


Fig. 9 (a) Synthesis of mesoporous chiral nematic bilayer PF resin films, which includes EISA process of two CNC layers and etching by alkaline solution. (b) Humidity-driven curling and uncurling of the bilayer PF film with concomitant color change. Reproduced with permission. Copyright 2014, Wiley-VCH Verlag GmbH & Co. KGaA, Weinheim. (c) Different modes of actuations of nematic CNC-based bilayer film. (d) Humidity-responsive mechanism of the nematic CNC-based bilayer film. (e) Collapse process of true (top) and biomimetic device (bottom) of *Mimosa pudica* leaf after touching. Reproduced with permission. Copyright 2018, the American Chemical Society. (f) CLCN film and protonated CLCN film prepared by direct ink writing in the dry and wet state. (g) Design principle of structural colored actuator by direct ink writing. (h) Demonstration of the heat and humidity-driven actuation of structural colored actuator by direct ink writing. Scale bar: 10 mm.

the bending and twisting deformation of the film could be realized by adjusting the tilt angle between the length of film and director of CNC nanorods because the nematic CNC layer provided mechanical anisotropy to the composite film (Fig. 9c and d).⁷⁴ Due to the mechanical anisotropy provided by the uniform-aligned CNC, diverse 3D motions could be triggered only by moisture of the palm and fingers of a human, as presented in Fig. 9e, enabling the CNC-based film to imitate biological motions of natural plants such as leaves of *Mimosa pudica*. 4D printing is an emerging technique to prepare stimuli-responsive materials by the 3D printing method, which is

considered a versatile strategy to fabricate functional soft matter *via* the bottom-up approach.^{67,85,86} Debijs and coworkers reported the fabrication of a humidity-responsive CLCN actuator using the 4D technique *via* an “aza-Michael” addition reaction.⁸⁷ The structural colored actuator was prepared by directly writing CLC oligomer inks on a plate, followed by warming the ink for a period of time to allow the mesogens to self-organize into a helical structure. The humidity-responsiveness was achieved by protonating the pendant amine groups in the matrix of CLCN by acid solution, as presented in Fig. 9f. Acidifying the whole CLCN film caused the matrix, as well as the helical pitch, to reversibly change, while acidifying only one side of the film endowed the with film humidity-responsive actuation ability (Fig. 9g and h). The material hosts, structure and actuation modes of LC-based humidity-responsive soft actuators are summarized in Table 1. The delicate material and structure design diversify the functionalities and application prospects of humidity-driven LC actuators.

4.2 Sensors and detectors

Taking advantage of the self-organized helical superstructure and hydrophilic property of CNC films or coatings, they can act as humidity sensors or indicators without further modification. Under different RH, the swelling ratio of CNC films is different, driving the change in the helical pitch of CNC according to the change in RH.^{88–90} In this case, the environmental RH is feasibly visualized by detecting the reflection band of the CNC film. Especially, finely tuning the reflection band over the visible wavelength range builds a relationship between structural colors and RH. However, pure CNC materials exhibit a poor mechanical performance and humidity-responsiveness.⁹¹ Thus, to broaden the practical applications of CNC materials, several pioneering works have been reported to prepare high-performance humidity-driven CNC materials by integrating functional elements in the CNC matrix. For example, Wang’s team used glycerol as a plasticizer and hygroscopic agent to improve the structural color tunability and mechanical toughness of the CNC matrix.⁹² Consequently, the iridescent color of the CNC film was totally modulable based on the doping concentration of glycerol. Moreover, obvious changes in the structural colors of the CNC film could be observed by changing the RH due to the water absorbing hygroscopic glycerol. An improvement in the mechanical properties and humidity sensitivity of CNCs could also be realized by incorporating hydrophilic polymer chains such as poly(ethylene glycol) (PEG),

Table 1 Representative soft actuators based on humidity-driven LC materials

Types	Structure/component	Actuation modes	Preparation	Ref.
LCN	Inhomogeneous alignment of hydrogen-bonded LC	Bend, curl	Radical polymerization	64 and 65
LCN	Inhomogeneous structure of hydrogen-bonded LCN	Bend, curl, twist	Radical polymerization	66 and 85
LCN	Inhomogeneous structure of amine-grafted LCN	Bend, curl, twist	Aza-Michael addition and radical polymerization	67 and 89
LCN	Bilayer of PA6 and LCN	Bend, twist	Radical polymerization	70 and 71
LCN	LCN with crosslink density gradient	Bend, twist, curl	Radical polymerization	68
LCN	Homogeneous azobenzene-doped LCN	Bend	Radical polymerization	83
LCN	Bilayer of hydrogel and LCN	Bend, twist	Radical polymerization	72
CNC	Sandwich structure of CNC layers and inner PA layer	Bend, twist	Evaporation-induced self-assembly	84
CNC	Bilayer of two CNC layers	Bend	Evaporation-induced self-assembly	42
CNC	Bilayer of CNC and porous polymer	Bend, twist	Evaporation-induced self-assembly	73
CNC	Bilayer of CNC and inverse opal structure	Bend, twist	Evaporation-induced self-assembly	74

poly(acrylic acid) and poly(vinyl alcohol) (PVA).^{47,93,94} Also, the humidity-responsive structural changes of the composite CNC film could be adjusted by the doping concentration, indicating the potential to fabricate usable humidity sensors with designable color changes. MacLachlan's group prepared a mesoporous and chiral nematic ordered phenol-formaldehyde (PF) resin film using a CNC template. As schematically illustrated in Fig. 10a, the film was obtained through the EISA process of CNC nanorods in PF solution, followed by etching the CNCs using alkaline solution. The flexibility and porosity of the polymer matrix made the film sensitive to humidity by presenting structural color changes.⁹⁴ As shown in Fig. 10b, due to the distinct swelling properties of the PF film in solvent, a visualized sensor was realized to detect the water content in ethanol. To improve the cycling stability of CNC photonic sensors, Lu and coworkers chemically linked polyacrylamide with CNC nanorods by glutaraldehyde through the reaction between the double aldehyde groups of the glutaraldehyde amino groups of polyacrylamide and hydroxyl groups of CNCs.⁹⁵ Due to the humidity sensitivity of the polyacrylamide chains, the CNC sensor was responsive to RH changes. As concluded in Fig. 10c, by suitably adjusting the doping ratio of polyacrylamide, the reflection band of the CNC film could change over 100 nm, and the corresponding colors varied from green to red when the RH changed from 11% to 97%, respectively. More importantly, the humidity-responsiveness of the CNC film was highly stable, which

could operate for 10 times without fatigue (Fig. 10d and e). To endow the humidity-driven CNC film with extra functionality, the thermo-responsive poly(*N*-isopropylacrylamide) (PNIPAM) was integrated in the CNC matrix and a humidity and heat dual responsive CNC film was realized.⁹⁶ The resulting CNC film not only presented humidity-responsive structural color changes due to the reversible changes of its helical pitch but was sensitive to the temperature due to the hydrophilic transition of PNIPAM around the lower critical solution temperature (LCST), as demonstrated in Fig. 10f. PNIPAM could be swollen when the surrounding temperature was lower than the LCST. By heating the material to a temperature above the LCST, shrinkage of PNIPAM occurred, driving shortening of the pitch of the CNC film, which endowed the dual-responsive CNC film potential for sensing and detecting RH and temperature.

Humidity-responsive LC materials are promising candidates for the fabrication of advanced sensors and detectors because of their superior advantages including easy preparation, high designability and programmability.^{97–99} Saha and coworkers reported the fabrication of a small-molar-weight CLC-based humidity sensor by doping a hydrolytically labile chiral molecule in the nematic LC E7.¹⁰⁰ After exposing the prepared CLC coating to humid air, the reflective color of CLC changed from blue to red within 5 min due to the decrease in the helical twisting power (HTP) of the chiral molecules after hydrolyzation. Different from the somewhat tedious EISA process required for the preparation of most of CNC films, polymeric LCN materials are suitable for diverse processing techniques and have high potential in wide application fields, ranging from humidity sensing to ion detection, gas detection and steam sterilization indication.^{101–104} Broer and coworkers reported the fabrication of a printable visualized humidity sensor based on hygroscopic CLCN coatings, which was capable of detecting RH within the range of 3% to 83%.³³ The carboxylic salty CLCN film was subsequently utilized for the detection of methanol and ethanol in a mixed solution.¹⁰⁵ As shown in Fig. 11a, in a solvent mixture of methanol, ethanol and water, the film presented reflective color changes when the ratio of methanol and ethanol varied due to the different affinities of the CLCN film with these two alcohol molecules. The affinity difference in the salty network and alcohols resulted in a distinct swelling ratio of the CLCN matrix when methanol or ethanol penetrated it. Based on the neutralization reaction between amine base and carboxylic acid, the same group prepared a gaseous trimethylamine detector, which functioned based on the synergistic effects of saltation of the hydrogen-bonded LCN and water-swelling of the salty network. The reflection band, as well as the reflective color of the CLCN detector changed when it was exposed to gaseous amine base under high RH.¹⁰⁶ More recently, our group prepared two acidic gas sensors based on an LCN actuator and CLCN film, respectively. The mechanism of the sensors was based on the reversible interaction between the LCN matrix and water and irreversible reaction between carboxylic salt with acid.¹⁰⁷ As shown in Fig. 11b, the LCN actuator showed reversible bending and unbending motions according to the changes in RH in the normal atmosphere. However, in an SO₂ atmosphere, the film remained still even with changes in RH.

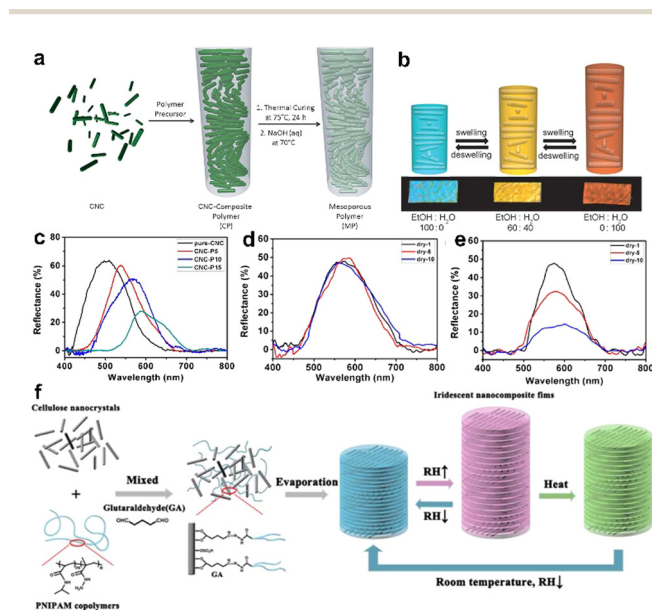


Fig. 10 (a) Illustration of the preparation of mesoporous chiral nematic PF resins. (b) Schematic representation of the swelling behavior of the mesoporous PF film and its reflective colors in mixtures of water and ethanol. Reproduced with permission. Copyright 2013, Wiley-VCH Verlag GmbH & Co. KGaA, Weinheim. (c) Reflectance spectra of CNC/polyacrylamide composite films with different polyacrylamide contents. Cycling tests of humidity-driven behavior of (d) CNC/polyacrylamide composites film and (e) pure CNC film. Reproduced with permission. Copyright 2019, the American Chemical Society. (f) Schematic illustration of preparation and humidity and heat dual responsive CNC/poly(*N*-isopropylacrylamide) composite film. Reproduced with permission. Copyright 2017, the American Chemical Society.

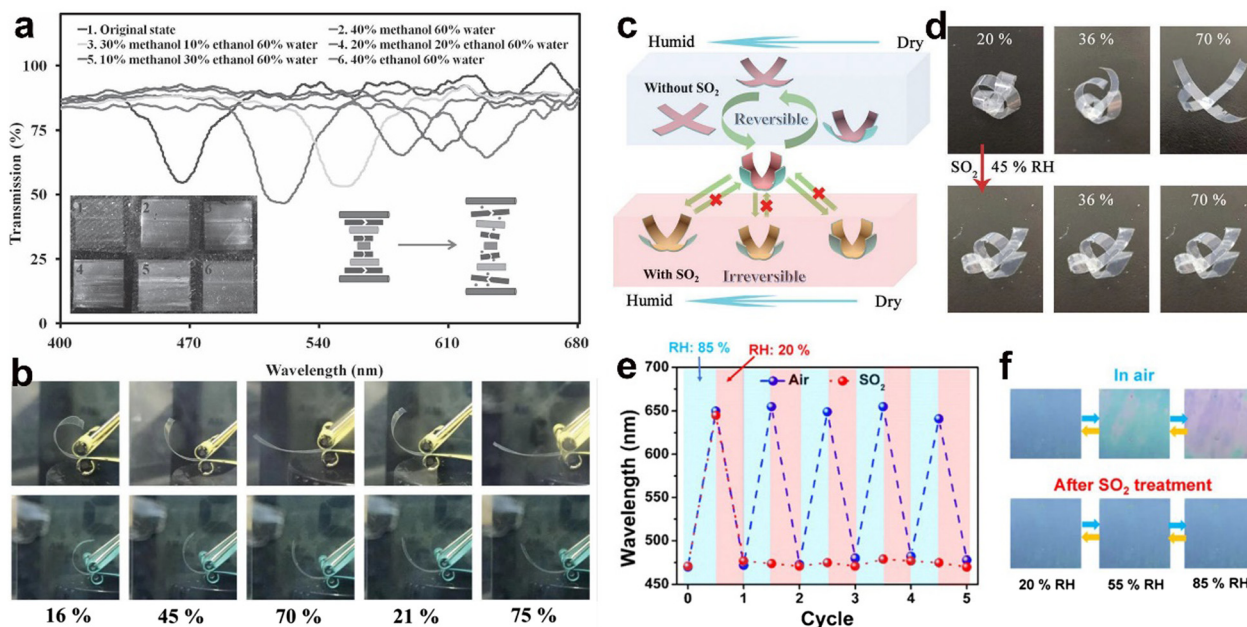


Fig. 11 (a) Reflection band changes of CLCN films as produced after breaking of the hydrogen bridges in alcohol solutions with different ethanol-methanol ratios. Reproduced with permission. Copyright 2012, Wiley-VCH Verlag GmbH & Co. KGaA, Weinheim. (b) Humidity-responsiveness of LCN film in normal atmosphere (top) and SO₂ atmosphere (bottom). (c) Schematic illustration and (d) real images of an artificial flower that mimics blooming and withering of natural flowers. Reproduced with permission. Copyright 2019, Wiley-VCH Verlag GmbH & Co. KGaA, Weinheim. Changes in (e) reflection center and (f) reflective color of humidity-responsive CLCN film in normal atmosphere and SO₂ atmosphere. Reproduced with permission. Copyright 2022, the American Chemical Society.

The humidity and SO₂ gas dual-responsive LCN actuator was prepared by alkalizing one side of a hydrogen-bonded LCN film, enabling inhomogeneous expansion between both sides of the film when the RH changed. When the film contacted SO₂ gas, the carboxylic salty group would be acidified and converted to non-hygroscopic carboxylic acid, terminating the humidity-responsiveness of the film. Thus, the concentration of SO₂ in the atmosphere could be estimated by the conversion time and RH. Using the SO₂-gated humidity-responsive LCN actuator, a biomimetic sensor that could detect acidic gas was prepared, as shown in Fig. 11c and d. The artificial flower bloomed and closed according to RH reversibly. When it detected SO₂ gas, the flower could not deform again, mimicking the wither of natural flowers. The SO₂ detector was further optimized by using a structural-colored CLCN matrix.¹⁰⁸ Consequently, the CLCN film showed reflection color changes from blue to red when the RH changed from 20% to 85%, while it became inert to humidity and remained blue when treated by SO₂ gas, indicating a visualized and power-free detector for acidic gas (Fig. 11e and f).

The design and synthesis of new building blocks by molecular engineering and improvement of material processing techniques have facilitated the advancement of humidity-driven LCN sensors. One of the main limitations of CLCN materials is the requirement of high-quality alignment techniques, seriously impeding their large-scale production and simplification of their preparation. BPLC possesses a 3D periodic nanostructure and reflective colors, which can be obtained by self-assembly without external aligning induction. Therefore, BPLC materials are considered promising candidates for the development of functional photonic devices.

However, due to the poor stability of the double-twisted cylinder (DTC) structure, BPLCs are generally formed in a narrow temperature range. Thus, to solve this challenge, Hu and coworkers synthesized a series of fluorinated LC monomers that showed an ultrawide BPLC temperature range.¹⁰⁹ By integrating a fluorinated BPLC with carboxylic acid dimer LC, a humidity-driven BPLC polymer was judiciously prepared.¹¹⁰ After alkalizing the BPLC, the matrix became hygroscopic. As shown in Fig. 12a, the reflective color of the BPLC was changeable from blue to red due to the dynamic lattice periods resulting from reversible water swelling, enabling the preparation of rewritable paper using water as ink. Moreover, the reflection wavelength of the BPLC changed over a wide range when the surrounding pH changed, indicating its potential in the fabrication of recyclable pH detectors (Fig. 12b). By incorporating a stretchable CLCN matrix with water-swallowable polymer, the applications of CLCN-based humidity sensors can be extended to wearable devices. Shi *et al.* prepared a visualized strain and humidity sensor by interpenetrating CLCN and hygroscopic poly(ampholyte).¹¹¹ As shown in Fig. 12c–e, the optical sensor could be integrated with cloth and detected motions in an easy-to-read way. Specifically, when it was directly attached to human skin, both motions of the human body and sweating of human skin could be detected by the obvious color changes. Besides molecular design and material preparation, the process technique is also important in the exploration of novel humidity-driven devices. Florea and coworkers fabricated a humidity-driven LCN micro-actuator using the direct laser writing technique.¹¹² As shown in Fig. 12f, the micrometer-scale LCN actuator was prepared by direct laser writing of a CLC photonic

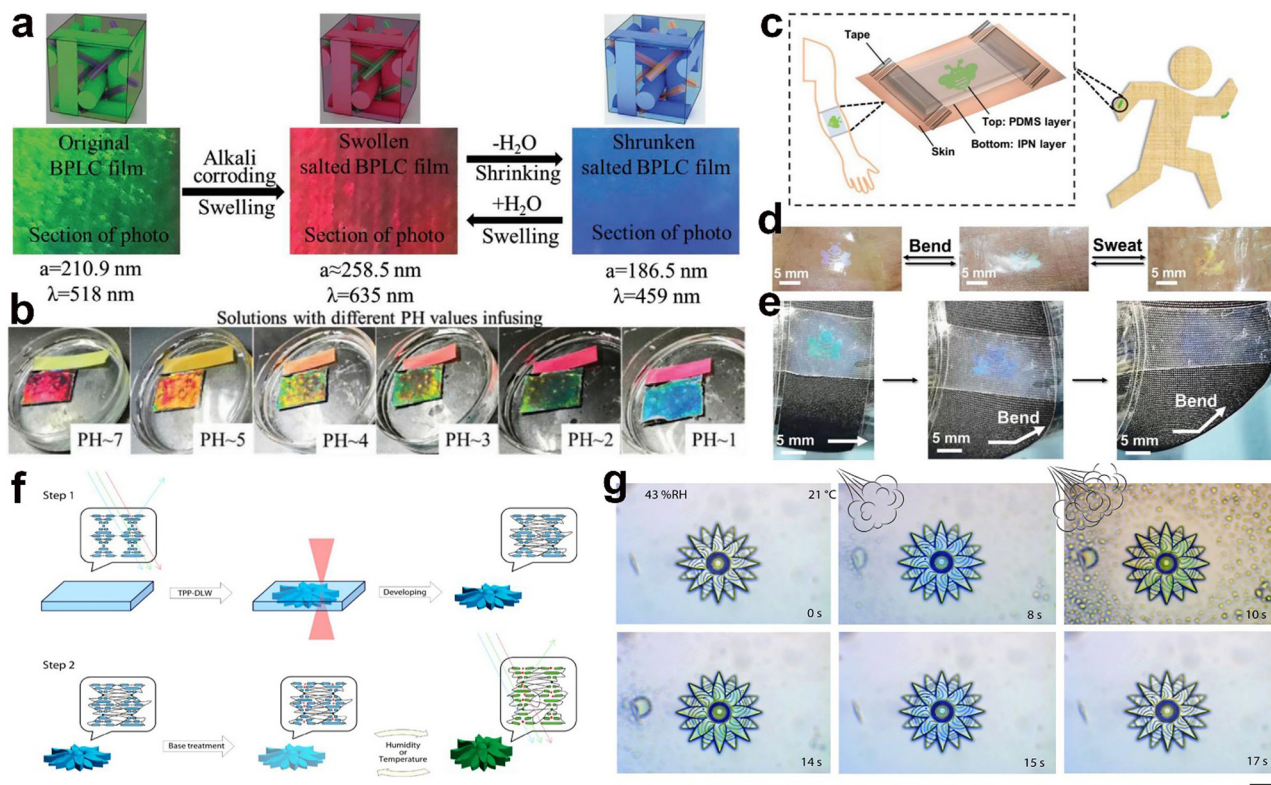


Fig. 12 (a) Schematic representation of mechanism of the humidity-responsiveness of a BPLC film and its reflective colors under different RH. (b) Photographs of the colors of the humidity-driven BPLC film in solutions with different pH values. Reproduced with permission. Copyright 2020, Wiley-VCH GmbH. (c) Schematic of wearable CLCN IPN sensors on the human body. (d) Reflective color change of the wearable sensor attached to a human body upon sweat exposure and bending motion. (e) Photographs showing the stretch-induced color changes of the bee pattern film attached to a human elbow. Reproduced with permission. Copyright 2021, Wiley-VCH GmbH. (f) Schematic of the fabrication and structure activation to obtain CLCN photonic micro-actuators. (g) Micrographs of the micro flower upon exposure to breath (top) and after (bottom). Reproduced with permission. Copyright 2020, the American Chemical Society.

precursor, followed by alkalinizing the actuator to make it hygroscopic. Consequently, the cholesteric actuator exhibited obvious structural color changes from blue to orange when treated with moisture (Fig. 12g). The color changing behavior was totally reversible after water evaporation, indicating that the dynamic changes of helical pitch could be realized even on the microscale.

Although reversibility and stability are important to evaluate the potential of functional materials, irreversible responsiveness is preferred in some application aspects such as monitoring handling history and conditions of preparation and transportation of materials.¹¹³ Schenning's group prepared a humidity-responsive CLCP coating that could evaluate steam sterilization by irreversible color changes.¹¹⁴ The crosslink-free CLCP was prepared by polymerizing mono-acrylate hydrogen-bonded monomers. When it was treated by steam at 120 °C for 20 min, the hydrogen bonds cleaved and the polymer turned from the ordered CLC state to isotropic state, causing the disappearance of the reflective color. The color change in the CLCP coating was irreversible due to the absence of a crosslinking network. This indicates that the CLCP coating retained the colorless state after cooling to room temperature. However, its color remained if the steam temperature and treating time did not reach a critical point. In this case, effective steam sterilization could be ensured

by simply observing the disappearance of the color in the CLCP detectors.

4.3 Other functional devices

Compared to freestanding materials, coatings are generally thin layers attached to a substrate. For stimuli-responsive shape-morphing coating, the confinement of the substrate limits the in-plane deformation, leading to striking shape changes in coating thickness.^{115–117} Humidity-responsive CLCN coatings operate by reversible swelling and shrinking due to water absorbing and desorbing, accompanied with an alteration in the topography of the coatings. Stumpel and coworkers investigated the thickness changes in a humidity-responsive hydrogen-bonded CLCN coating.¹¹⁸ Due to the thermochromic property of the hydrogen-bonded CLC matrix, a patterned coating could be prepared *via* the stepwise polymerization of different regions at distinct temperatures. As shown in Fig. 13a and 14b, water swelling resulted in a micrometer-scale thickness change in a specific region. Also, the reflection color was totally related to the film thickness due to the changes in the helical pitch. In this case, a water-responsive colorful display was realized (Fig. 13c). Schenning's group achieved humidity-directed colorful paint using ions as physical crosslinks.⁵⁸ As shown in Fig. 13d, treating the film with different

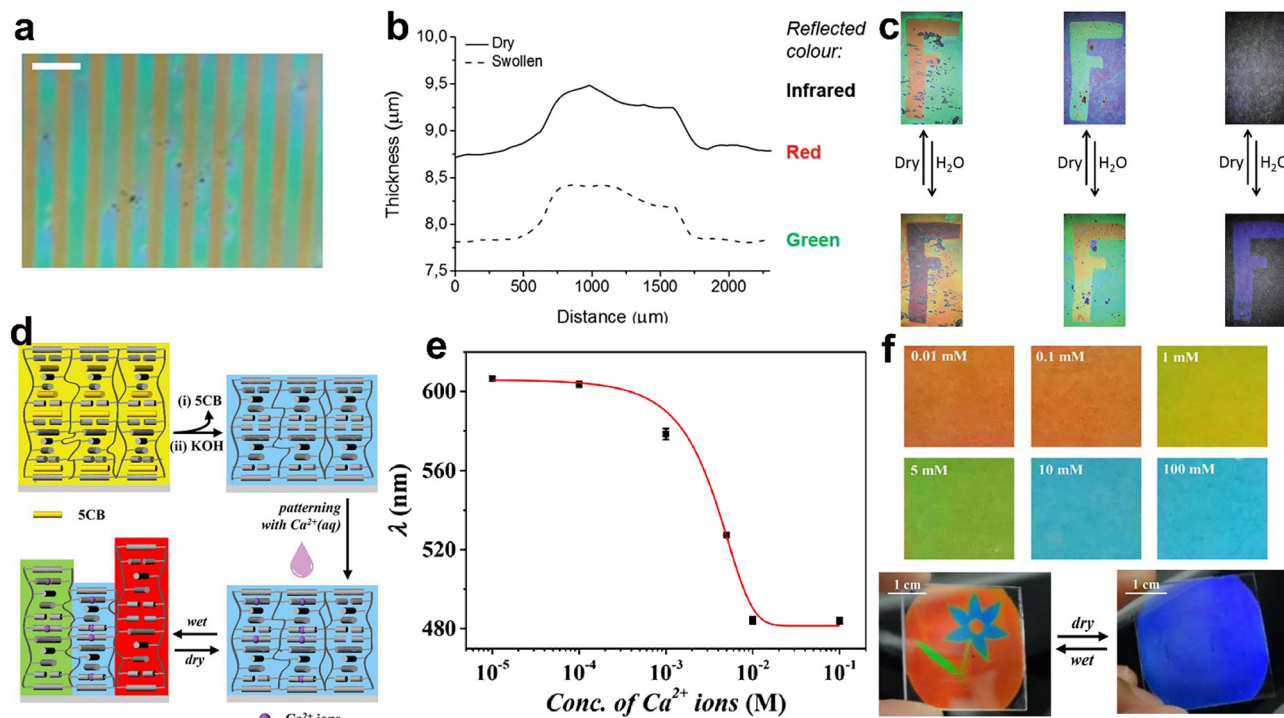


Fig. 13 (a) Optical image of a patterned CLCN coating. The scale bar represents 3 mm. (b) Thickness of the coating under different RH and the corresponding reflective colors. (c) Humidity-responsive color changeable “F”-patterned CLCN coating. Reproduced with permission. Copyright 2015, The Royal Society of Chemistry. (d) Schematic of the preparation and working principle of the ion-crosslinked CLCN coating. (e) Changes of reflection center of CLCN coating when immersed in solution with different concentrations of Ca^{2+} ions. (f) Reflective color of CLCN coating when treated by different concentrations of Ca^{2+} ions. (g) Reversible appearance and disappearance of ion-crosslinked CLCN coating. Reproduced with permission. Copyright 2018, the American Chemical Society.

concentrations of ions led to tunable humidity responsiveness. The color-changing ability was adjustable due to the degree of ionic crosslinking (Fig. 13e). By controlling the regional crosslinking degree, words or pictures could be written on the CLCN film. The information only appeared under high RH, while it disappeared under low RH, indicating its potential applications in smart decoration and information encryption, as shown in Fig. 13f. Given that the humidity-driven color-change ability is similar to that of some biological behaviors, Wang's team exploited creature-like camouflage devices using humidity-responsive BPLC coatings.¹¹⁹ The coating presented green reflection color under low RH, while showed red color when the RH increased. Acting as artificial skin, the color changing behaviors of the natural longhorn beetle could be imitated. Also, a colorimetric sensor for fruits was realized by simply attaching the coating on a package, providing real-time testing of the freshness of the fruits.

Although the visible color changing behaviors of CLCN and CNCs have been widely researched and utilized in diverse application fields, a single functionality is not sufficient to satisfy the requirements of complex systems. Fluorescence can only be observed by excitation from external light irradiation, presenting potential in information encryption and anti-counterfeiting. Recently, the incorporation of fluorescence in humidity-driven LC systems has been considered as an intriguing and effective strategy for the fabrication of advanced

humidity-driven LC materials. Interestingly, there are plenty of interactions between chiral LC materials and fluorescence. For example, chiral LCs including CNCs, CLC and CLCN have been widely researched as a soft template to induce circularly polarized luminescence.¹²⁰ Deng's team reported a humidity-responsive fluorescent dansyl-grafted polymer co-assembled CNC film with dynamic circularly polarized emissions.¹²¹ A change in RH caused the film to show a structural color change in the full visible light wavelength range due to the reversible swelling and shrinking of the CNC matrix. The dynamic pitch changes led to the corresponding wavelength variation in the CPL emissions. More recently, our team prepared a new CLCN film showing visible and fluorescent dual patterns controlled solely by humidity changes.⁵⁹ The CLCN coating was prepared by chemically bonding hydrochromic fluorescent molecules in a humidity-responsive CLCN film. By ionic locking, the CLCN matrix became non-hygroscopic and water molecules could not penetrate in the network, providing chances to construct arbitrary patterns in the CLCN film by partially crosslinking the matrix. As presented in Fig. 14a, the ionically crosslinked CLCN coating showed uniform structural color and fluorescence under a normal atmosphere. By wetting the film by human breath, both of a visible pattern and fluorescent pattern appeared simultaneously (Fig. 14b). However, only one set of information could be written in the film using this method. Thus, to explore free-standing materials that present distinct visible and fluorescence

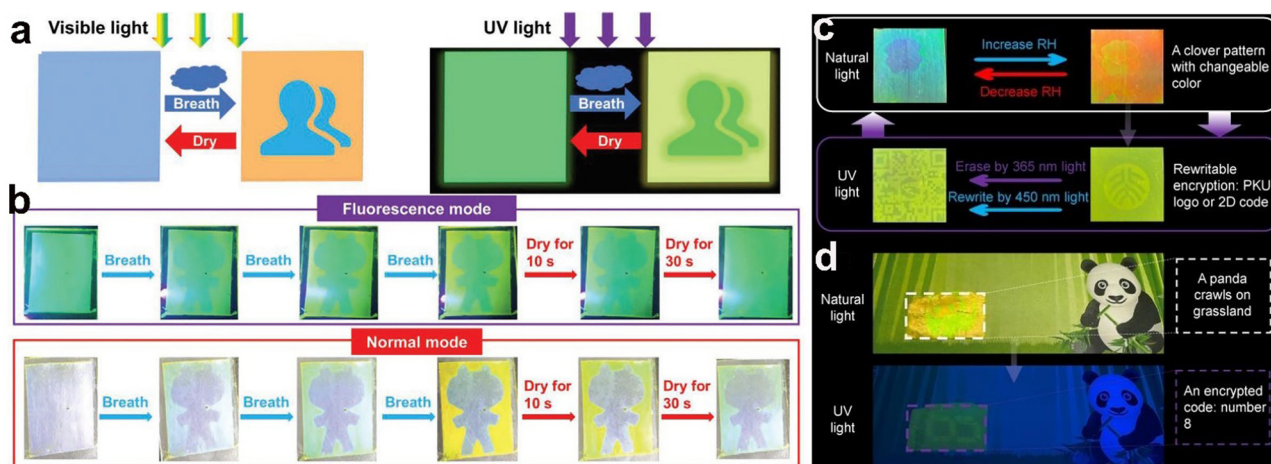


Fig. 14 (a) Schematic illustration and (b) real images of humidity-responsive anti-counterfeiting devices showing visible and fluorescent changes. Reproduced with permission. Copyright 2021, Wiley-VCH GmbH. (c) Distinct visible and fluorescent information encrypted in a single CLCN film. (d) Information encryption in the novel CLCN film. Reproduced with permission. Copyright 2022, Wiley-VCH GmbH.

information, very recently, a polymerizable hydrazone photo-switch was designed and synthesized.¹²² By bonding a hydrazone photo-switch in a humidity-driven CLCN film, two distinct sets of information could be encrypted in a single film, which could be read out in reflective mode and emissive mode, respectively. As presented in Fig. 14c, a hydrochromic pattern and a distinct fluorescent pattern could be integrated in a single CLCN film without interference. Using this novel responsive film, information encryption was realized, as shown in Fig. 14d. The film exhibited a panda pattern in visible light. However, the encrypted information as a number 8 could only be read using UV light.

5. Conclusion and outlook

Humidity-driven LC materials are a class of emerging functional materials for the design and fabrication of harmlessly controlled soft robots and humidity sensors. The development of advanced humidity-responsive LC materials is meaningful for the exploration of autonomous shape-shifting actuators that continuously convert environmental RH changes into mechanical output given that humidity changes are instantaneous. The programmable molecular alignment and sensitivity of self-organized LC host allow the adaptive functionality of humidity-driven LC actuators, facilitating the construction of power-free smart robots and intelligent systems. Moreover, these materials also present opportunities for the construction of usable sensors and detectors that can sense the surrounding conditions such as humidity, temperature and other chemicals in a power-free way. The sensing and detecting results are easily read out by performing visible color changes, indicating the potential of these materials in industrial applications. Compared to some conventional actuators and sensors, which are only sensitive to harsh stimulations including UV light, high temperature, metal ions and strong acid or base, the harmlessness of moisture makes these emerging materials highly desirable in biomedical applications, such as drug delivery, wound healing and even tumor therapy.

In this review, we provided a comprehensive summary of the development and recent progress of humidity-driven LC materials. To date, efforts have been devoted to exploiting high-performance humidity-driven LC materials based on various mechanisms including hydrogen bonding, electrostatic interaction, and hydrophilic effect. To broaden the application prospects and complexify functionalities of these intriguing materials, diverse fabrication strategies have been developed, such as construction of inhomogeneous structures, bilayer strategies and IPN methods. The humidity-driven LC materials have been proven to be effective in application fields ranging from self-adaptive soft robots, visualized sensors and detectors to dynamic surface and biomimetic devices.

However, based on the current status, most humidity-driven LCP and CNC films operate only under high RH (higher than 50% RH) due to their poor water-absorbing ability under low RH. Thus, improving the sensitivity of humidity-responsive LC materials to RH changes especially under low RH is desirable for the development of next-generation functional devices. Furthermore, integrating multiple functionalities into a single material to mimic complicated creature-like behaviors is still in its infancy. This obstacle should be overcome by systematic design from molecular engineering to hierarchical construction because it is rarely possible to add extra functions to existing humidity-driven LC systems by simply physical mixing of distinct components or moieties. Thirdly, the enhancement of the stability and robustness of humidity-responsive LC devices is the next goal to facilitate their real applications. To achieve this, exploring new material matrices and optimizing the fabrication techniques are both required. Finally, challenges are opportunities, and thus it is believed that humidity-responsive LC materials have potential and can inspire the fabrication of next-generation functional smart matter.

Author contributions

R. Lan, H. Yang contribute to the conceptualization of the work. R. Lan, W. Shen and W. Yao contribute to the writing of

manuscript. R. Lan, W. Yao and H. Yang contribute to the funding acquisition. J. Chen and X. Chen contribute to the revision of the manuscript.

Conflicts of interest

There are no conflicts to declare.

Acknowledgements

This work was supported by the National Natural Science Foundation of China (Grant No. 52202081 and 52263033), China Postdoctoral Science Foundation Funded Project (No. BX2021003 and 2022M720206) and Natural Science Foundation of Gansu Province (Grant No. 20JR10RA105).

Notes and references

- Y. Forterre, J. M. Skotheim, J. Dumais and L. Mahadevan, How the Venus flytrap snaps, *Nature*, 2005, **433**, 421–425.
- I. Burgert and P. Fratzl, Actuation systems in plants as prototypes for bioinspired devices, *Philos. Trans. R. Soc., A*, 2009, **367**, 1541–1557.
- R. Elbaum, L. Zaltzman, I. Burgert and P. Fratzl, The Role of Wheat Awns in the Seed Dispersal Unit, *Science*, 2007, **316**, 884–886.
- L. Goswami, J. W. C. Dunlop, K. Jungnikl, M. Eder, N. Gierlinger, C. Coutand, G. Jeronimidis, P. Fratzl and I. Burgert, Stress generation in the tension wood of poplar is based on the lateral swelling power of the G-layer, *Plant J.*, 2008, **56**, 531–538.
- P. Fratzl and F. G. Barth, Biomaterial systems for mechanosensing and actuation, *Nature*, 2009, **462**, 442–448.
- J. W. C. Dunlop, R. Weinkamer and P. Fratzl, Artful interfaces within biological materials, *Mater. Today*, 2011, **14**, 70–78.
- L. Ionov, Biomimetic Hydrogel-Based Actuating Systems, *Adv. Funct. Mater.*, 2013, **23**, 4555–4570.
- C. Dawson, J. F. V. Vincent and A.-M. Rocca, How pine cones open, *Nature*, 1997, **390**, 668.
- Z. Aytac, J. Xu, S. K. Raman Pillai, B. D. Eitzer, T. Xu, N. Vaze, K. W. Ng, J. C. White, M. B. Chan-Park, Y. Luo and P. Demokritou, Enzyme- and Relative Humidity-Responsive Antimicrobial Fibers for Active Food Packaging, *ACS Appl. Mater. Interfaces*, 2021, **13**, 50298–50308.
- R. Qu, W. Zhang, X. Li, Y. Liu, Y. Wei, L. Feng and L. Jiang, Peanut Leaf-Inspired Hybrid Metal–Organic Framework with Humidity-Responsive Wettability: toward Controllable Separation of Diverse Emulsions, *ACS Appl. Mater. Interfaces*, 2020, **12**, 6309–6318.
- Y. Park and X. Chen, Water-responsive materials for sustainable energy applications, *J. Mater. Chem. A*, 2020, **8**, 15227–15244.
- J. Shen, B. Luan, H. Pei, Z. Yang, X. Zuo, G. Liu, J. Shi, L. Wang, R. Zhou, W. Cheng and C. Fan, Humidity-Responsive Single-Nanoparticle-Layer Plasmonic Films, *Adv. Mater.*, 2017, **29**, 1606796.
- E. Castellón, M. Zayat and D. Levy, Novel Reversible Humidity-Responsive Light Transmission Hybrid Thin-Film Material Based on a Dispersive Porous Structure with Embedded Hygroscopic and Deliquescent Substances, *Adv. Funct. Mater.*, 2018, **28**, 1704717.
- H. Lin, J. Gong, M. Eder, R. Schuetz, H. Peng, J. W. C. Dunlop and J. Yuan, Programmable Actuation of Porous Poly(Ionic Liquid) Membranes by Aligned Carbon Nanotubes, *Adv. Mater. Interfaces*, 2017, **4**, 1600768.
- Y. Ge, R. Cao, S. Ye, Z. Chen, Z. Zhu, Y. Tu, D. Ge and X. Yang, A bio-inspired homogeneous graphene oxide actuator driven by moisture gradients, *Chem. Commun.*, 2018, **54**, 3126–3129.
- J. Troyano, A. Carné-Sánchez and D. MasPOCH, Programmable Self-Assembling 3D Architectures Generated by Patterning of Swellable MOF-Based Composite Films, *Adv. Mater.*, 2019, **31**, 1808235.
- L. Zhang and P. Naumov, Light- and Humidity-Induced Motion of an Acidochromic Film, *Angew. Chem., Int. Ed.*, 2015, **54**, 8642–8647.
- E. S. Muckley, M. Naguib and I. N. Ivanov, Multi-modal, ultrasensitive, wide-range humidity sensing with Ti₃C₂ film, *Nanoscale*, 2018, **10**, 21689–21695.
- W. Pu, F. Wei, L. Yao and S. Xie, A review of humidity-driven actuator: toward high response speed and practical applications, *J. Mater. Sci.*, 2022, **57**, 12202–12235.
- J. Wang, H. Ma, Y. Liu, Z. Xie and Z. Fan, MXene-Based Humidity-Responsive Actuators: Preparation and Properties, *ChemPlusChem*, 2021, **86**, 406–417.
- H. Arazoe, D. Miyajima, K. Akaike, F. Araoka, E. Sato, T. Hikima, M. Kawamoto and T. Aida, An autonomous actuator driven by fluctuations in ambient humidity, *Nat. Mater.*, 2016, **15**, 1084–1089.
- H. K. Bisoyi and Q. Li, Liquid Crystals: Versatile Self-Organized Smart Soft Materials, *Chem. Rev.*, 2022, **122**, 4887–4926.
- Y. Yang, L. Wang, H. Yang and Q. Li, 3D Chiral Photonic Nanostructures Based on Blue-Phase Liquid Crystals, *Small, Science*, 2021, **1**, 2100007.
- D. J. Broer, J. Boven, G. N. Mol and G. Challa, In-situ photopolymerization of oriented liquid-crystalline acrylates, 3. Oriented polymer networks from a mesogenic diacrylate, *Die Makromolekulare Chemie*, 1989, **190**, 2255–2268.
- H. Finkelmann, W. Gleim, K. Hammerschmidt and J. Schätzle, Liquid crystal elastomers, *Makromol. Chem., Macromol. Symp.*, 1989, **26**, 67.
- E. M. Terentjev, Liquid-crystalline elastomers, *J. Phys.: Condens. Matter*, 1999, **11**, R239–R257.
- J. Yang, X. Zhang, X. Zhang, L. Wang, W. Feng and Q. Li, Beyond the Visible: Bioinspired Infrared Adaptive Materials, *Adv. Mater.*, 2021, **33**, 2004754.
- D.-Y. Kim, C. Nah, S.-W. Kang, S. H. Lee, K. M. Lee, T. J. White and K.-U. Jeong, Free-Standing and Circular-

- Polarizing Chirophotonic Crystal Reflectors: Photopolymerization of Helical Nanostructures, *ACS Nano*, 2016, **10**, 9570–9576.
- 29 J. Bao, Z. Wang, C. Shen, R. Huang, C. Song, Z. Li, W. Hu, R. Lan, L. Zhang and H. Yang, Freestanding Helical Nanostructured Chiro-Photonic Crystal Film and Anticounterfeiting Label Enabled by a Cholesterol-Grafted Light-Driven Molecular Motor, *Small Methods*, 2022, **6**, 2200269.
 - 30 P. Zhang, X. Shi, A. P. H. J. Schenning, G. Zhou and L. T. de Haan, A Patterned Mechanochromic Photonic Polymer for Reversible Image Reveal, *Adv. Mater. Interfaces*, 2020, **7**, 1901878.
 - 31 E. P. A. van Heeswijk, L. Yang, N. Grossiord and A. P. H. J. Schenning, Tunable Photonic Materials via Monitoring Step-Growth Polymerization Kinetics by Structural Colors, *Adv. Funct. Mater.*, 2020, **30**, 1906833.
 - 32 W. Yao, R. Lan, K. Li and L. Zhang, Multiple Anti-Counterfeiting Composite Film Based on Cholesteric Liquid Crystal and QD Materials, *ACS Appl. Mater. Interfaces*, 2021, **13**, 1424–1430.
 - 33 N. Herzer, H. Guneyasu, D. J. D. Davies, D. Yildirim, A. R. Vaccaro, D. J. Broer, C. W. M. Bastiaansen and A. P. H. J. Schenning, Printable Optical Sensors Based on H-Bonded Supramolecular Cholesteric Liquid Crystal Networks, *J. Am. Chem. Soc.*, 2012, **134**, 7608–7611.
 - 34 Y. Habibi, L. A. Lucia and O. J. Rojas, Cellulose Nanocrystals: Chemistry, Self-Assembly, and Applications, *Chem. Rev.*, 2010, **110**, 3479–3500.
 - 35 R. J. Moon, A. Martini, J. Nairn, J. Simonsen and J. Youngblood, Cellulose nanomaterials review: structure, properties and nanocomposites, *Chem. Soc. Rev.*, 2011, **40**, 3941–3994.
 - 36 D. Klemm, B. Heublein, H.-P. Fink and A. Bohn, Cellulose: Fascinating Biopolymer and Sustainable Raw Material, *Angew. Chem., Int. Ed.*, 2005, **44**, 3358–3393.
 - 37 S. Hu, S. Wu, C. Li, R. Chen, E. Forsberg and S. He, SNR-enhanced temperature-insensitive microfiber humidity sensor based on upconversion nanoparticles and cellulose liquid crystal coating, *Sens. Actuators, B*, 2020, **305**, 127517.
 - 38 M. K. Khan, W. Y. Hamad and M. J. MacLachlan, Tunable Mesoporous Bilayer Photonic Resins with Chiral Nematic Structures and Actuator Properties, *Adv. Mater.*, 2014, **26**, 2323–2328.
 - 39 Y. Cao, P.-X. Wang, F. D'Acierno, W. Y. Hamad, C. A. Michal and M. J. MacLachlan, Tunable Diffraction Gratings from Biosourced Lyotropic Liquid Crystals, *Adv. Mater.*, 2020, **32**, 1907376.
 - 40 R. Chen, D. Feng, G. Chen, X. Chen and W. Hong, Re-Printable Chiral Photonic Paper with Invisible Patterns and Tunable Wettability, *Adv. Funct. Mater.*, 2021, **31**, 2009916.
 - 41 P. Lv, X. Lu, L. Wang and W. Feng, Nanocellulose-Based Functional Materials: From Chiral Photonics to Soft Actuator and Energy Storage, *Adv. Funct. Mater.*, 2021, **31**, 2104991.
 - 42 W. Ge, F. Zhang, D. Wang, Q. Wei, Q. Li, Z. Feng, S. Feng, X. Xue, G. Qing and Y. Liu, Highly Tough, Stretchable, and Solvent-Resistant Cellulose Nanocrystal Photonic Films for Mechanochromism and Actuator Properties, *Small*, 2022, **18**, 2107105.
 - 43 O. Kose, A. Tran, L. Lewis, W. Y. Hamad and M. J. MacLachlan, Unwinding a spiral of cellulose nanocrystals for stimuli-responsive stretchable optics, *Nat. Commun.*, 2019, **10**, 510.
 - 44 M. Xu, W. Li, C. Ma, H. Yu, Y. Wu, Y. Wang, Z. Chen, J. Li and S. Liu, Multifunctional chiral nematic cellulose nanocrystals/glycerol structural colored nanocomposites for intelligent responsive films, photonic inks and iridescent coatings, *J. Mater. Chem. C*, 2018, **6**, 5391–5400.
 - 45 C. M. Walters, C. E. Boott, T.-D. Nguyen, W. Y. Hamad and M. J. MacLachlan, Iridescent Cellulose Nanocrystal Films Modified with Hydroxypropyl Cellulose, *Biomacromolecules*, 2020, **21**, 1295–1302.
 - 46 K. Yao, Q. Meng, V. Bulone and Q. Zhou, Flexible and Responsive Chiral Nematic Cellulose Nanocrystal/Poly(ethylene glycol) Composite Films with Uniform and Tunable Structural Color, *Adv. Mater.*, 2017, **29**, 1701323.
 - 47 J. A. Kelly, A. M. Shukaliak, C. C. Y. Cheung, K. E. Shopsowitz, W. Y. Hamad and M. J. MacLachlan, Responsive Photonic Hydrogels Based on Nanocrystalline Cellulose, *Angew. Chem., Int. Ed.*, 2013, **52**, 8912–8916.
 - 48 D. Trache, M. H. Hussin, M. K. M. Haafiz and V. K. Thakur, Recent progress in cellulose nanocrystals: sources and production, *Nanoscale*, 2017, **9**, 1763–1786.
 - 49 Y. Ma and J. Sun, Humido- and Thermo-Responsive Free-Standing Films Mimicking the Petals of the Morning Glory Flower, *Chem. Mater.*, 2009, **21**, 898–902.
 - 50 F. Gao, N. Zhang, X. Fang and M. Ma, Magnetically directed soft actuators driven by moisture, *J. Mater. Chem. C*, 2017, **5**, 4129–4133.
 - 51 D.-D. Han, Y.-L. Zhang, Y. Liu, Y.-Q. Liu, H.-B. Jiang, B. Han, X.-Y. Fu, H. Ding, H.-L. Xu and H.-B. Sun, Bioinspired Graphene Actuators Prepared by Unilateral UV Irradiation of Graphene Oxide Papers, *Adv. Funct. Mater.*, 2015, **25**, 4548–4557.
 - 52 Y. Liu, B. Xu, S. Sun, J. Wei, L. Wu and Y. Yu, Humidity- and Photo-Induced Mechanical Actuation of Cross-Linked Liquid Crystal Polymers, *Adv. Mater.*, 2017, **29**, 1604792.
 - 53 G. Zhao, Y. Huang, C. Mei, S. Zhai, Y. Xuan, Z. Liu, M. Pan and O. J. Rojas, Chiral Nematic Coatings Based on Cellulose Nanocrystals as a Multiplexing Platform for Humidity Sensing and Dual Anticounterfeiting, *Small*, 2021, **17**, 2103936.
 - 54 C. Mellot-Draznieks, C. Serre, S. Surblé, N. Audebrand and G. Férey, Very Large Swelling in Hybrid Frameworks: A Combined Computational and Powder Diffraction Study, *J. Am. Chem. Soc.*, 2005, **127**, 16273–16278.
 - 55 J. Troyano, A. Carné-Sánchez, J. Pérez-Carvajal, L. León-Reina, I. Imaz, A. Cabeza, D. Maspoch and A. Self-Folding, Polymer Film Based on Swelling Metal–Organic Frameworks, *Angew. Chem., Int. Ed.*, 2018, **57**, 15420–15424.
 - 56 Y. He, J. Guo, X. Yang, B. Guo and H. Shen, Highly sensitive humidity-driven actuators based on metal–organic frameworks incorporating thermoplastic polyurethane with gradient polymer distribution, *RSC Adv.*, 2021, **11**, 37744–37751.

- 57 J. E. Stumpel, E. R. Gil, A. B. Spoelstra, C. W. M. Bastiaansen, D. J. Broer and A. P. H. J. Schenning, Stimuli-Responsive Materials Based on Interpenetrating Polymer Liquid Crystal Hydrogels, *Adv. Funct. Mater.*, 2015, **25**, 3314–3320.
- 58 M. Moirangthem and A. P. H. J. Schenning, Full Color Camouflage in a Printable Photonic Blue-Colored Polymer, *ACS Appl. Mater. Interfaces*, 2018, **10**, 4168–4172.
- 59 R. Lan, Q. Wang, C. Shen, R. Huang, J. Bao, Z. Zhang, L. Zhang and H. Yang, Humidity-Induced Simultaneous Visible and Fluorescence Photonic Patterns Enabled by Integration of Covalent Bonds and Ionic Crosslinks, *Adv. Funct. Mater.*, 2021, **31**, 2106419.
- 60 I. K. Shishmanova, C. W. M. Bastiaansen, A. P. H. J. Schenning and D. J. Broer, Two-dimensional pH-responsive printable smectic hydrogels, *Chem. Commun.*, 2012, **48**, 4555–4557.
- 61 K. M. Lee, T. J. Bunning and T. J. White, Autonomous, Hands-Free Shape Memory in Glassy, Liquid Crystalline Polymer Networks, *Adv. Mater.*, 2012, **24**, 2839–2843.
- 62 L. T. de Haan, V. Gimenez-Pinto, A. Konya, T.-S. Nguyen, J. M. N. Verjans, C. Sánchez-Somolinos, J. V. Selinger, R. L. B. Selinger, D. J. Broer and A. P. H. J. Schenning, Accordion-like Actuators of Multiple 3D Patterned Liquid Crystal Polymer Films, *Adv. Funct. Mater.*, 2014, **24**, 1251–1258.
- 63 S. Iamsaard, S. J. Aßhoff, B. Matt, T. Kudernac, J. J. L. M. Cornelissen, S. P. Fletcher and N. Katsonis, Conversion of light into macroscopic helical motion, *Nat. Chem.*, 2014, **6**, 229–235.
- 64 O. M. Wani, R. Verpaalen, H. Zeng, A. Priimagi and A. P. H. J. Schenning, An Artificial Nocturnal Flower via Humidity-Gated Photoactuation in Liquid Crystal Networks, *Adv. Mater.*, 2019, **31**, 1805985.
- 65 K. D. Harris, C. W. M. Bastiaansen, J. Lub and D. J. Broer, Self-Assembled Polymer Films for Controlled Agent-Driven Motion, *Nano Lett.*, 2005, **5**, 1857–1860.
- 66 L. T. de Haan, J. M. N. Verjans, D. J. Broer, C. W. M. Bastiaansen and A. P. H. J. Schenning, Humidity-Responsive Liquid Crystalline Polymer Actuators with an Asymmetry in the Molecular Trigger That Bend, Fold, and Curl, *J. Am. Chem. Soc.*, 2014, **136**, 10585–10588.
- 67 K. Kim, Y. Guo, J. Bae, S. Choi, H. Y. Song, S. Park, K. Hyun and S.-K. Ahn, 4D Printing of Hygroscopic Liquid Crystal Elastomer Actuators, *Small*, 2021, **17**, 2100910.
- 68 A. Ryabchun, F. Lancia, A.-D. Nguindjel and N. Katsonis, Humidity-responsive actuators from integrating liquid crystal networks in an orienting scaffold, *Soft Matter*, 2017, **13**, 8070–8075.
- 69 Y. Chen, J. Yang, X. Zhang, Y. Feng, H. Zeng, L. Wang and W. Feng, Light-driven bimorph soft actuators: design, fabrication, and properties, *Mater. Horiz.*, 2021, **8**, 728–757.
- 70 M. Dai, O. T. Picot, J. M. N. Verjans, L. T. de Haan, A. P. H. J. Schenning, T. Peijs and C. W. M. Bastiaansen, Humidity-Responsive Bilayer Actuators Based on a Liquid-Crystalline Polymer Network, *ACS Appl. Mater. Interfaces*, 2013, **5**, 4945–4950.
- 71 R. C. P. Verpaalen, M. G. Debye, C. W. M. Bastiaansen, H. Halilović, T. A. P. Engels and A. P. H. J. Schenning, Programmable helical twisting in oriented humidity-responsive bilayer films generated by spray-coating of a chiral nematic liquid crystal, *J. Mater. Chem. A*, 2018, **6**, 17724–17729.
- 72 R. Lan, Y. Gao, C. Shen, R. Huang, J. Bao, Z. Zhang, Q. Wang, L. Zhang and H. Yang, Humidity-Responsive Liquid Crystalline Network Actuator Showing Synergistic Fluorescence Color Change Enabled by Aggregation Induced Emission Luminogen, *Adv. Funct. Mater.*, 2021, **31**, 2101578.
- 73 M. Wang, X. Tian, R. H. A. Ras and O. Ikkala, Sensitive Humidity-Driven Reversible and Bidirectional Bending of Nanocellulose Thin Films as Bio-Inspired Actuation, *Adv. Mater. Interfaces*, 2015, **2**, 1500080.
- 74 Q. Zhu, Y. Jin, W. Wang, G. Sun and D. Wang, Bioinspired Smart Moisture Actuators Based on Nanoscale Cellulose Materials and Porous, Hydrophilic EVOH Nanofibrous Membranes, *ACS Appl. Mater. Interfaces*, 2019, **11**, 1440–1448.
- 75 X. Li, J. Liu, D. Li, S. Huang, K. Huang and X. Zhang, Bioinspired Multi-Stimuli Responsive Actuators with Synergistic Color- and Morphing-Change Abilities, *Adv. Sci.*, 2021, **8**, 2101295.
- 76 T. Ube, K. Minagawa and T. Ikeda, Interpenetrating polymer networks of liquid-crystalline azobenzene polymers and poly(dimethylsiloxane) as photomobile materials, *Soft Matter*, 2017, **13**, 5820–5823.
- 77 K. Takado, T. Ube and T. Ikeda, Photomobile Polymer Materials with Double Network Structures: Crosslinked Azobenzene Liquid-Crystalline Polymer/Methacrylate Composites, *Mol. Cryst. Liq. Cryst.*, 2014, **601**, 43–48.
- 78 T. Ube, Development of novel network structures in cross-linked liquid-crystalline polymers, *Polym. J.*, 2019, **51**, 983–988.
- 79 H.-F. Lu, M. Wang, X.-M. Chen, B.-P. Lin and H. Yang, Interpenetrating Liquid-Crystal Polyurethane/Polyacrylate Elastomer with Ultrastrong Mechanical Property, *J. Am. Chem. Soc.*, 2019, **141**, 14364–14369.
- 80 Z. Deng, G. Zhou and L. T. de Haan, Preparation of an Interpenetrating Network of a Poly(ampholyte) and a Cholesteric Polymer and Investigation of Its Hydrochromic Properties, *ACS Appl. Mater. Interfaces*, 2019, **11**, 36044–36051.
- 81 L. Zhang, W. He, Y. Cui, Y. Zhang, Z. Yang, D. Wang, H. Cao and Y. Li, Preparation and properties of water-responsive films with color controllable based on liquid crystal and poly(ethylene glycol) interpenetrating polymer network, *Liq. Cryst.*, 2022, **49**, 1411–1419.
- 82 K.-G. Noh and S.-Y. Park, Biosensor Array of Interpenetrating Polymer Network with Photonic Film Templated from Reactive Cholesteric Liquid Crystal and Enzyme-Immobilized Hydrogel Polymer, *Adv. Funct. Mater.*, 2018, **28**, 1707562.
- 83 T. Wu, J. Li, J. Li, S. Ye, J. Wei and J. Guo, A bio-inspired cellulose nanocrystal-based nanocomposite photonic film

- with hyper-reflection and humidity-responsive actuator properties, *J. Mater. Chem. C*, 2016, **4**, 9687–9696.
- 84 Z. Wang, R. Lan, J. Bao, C. Shen, R. Huang, C. Song, L. Zhang and H. Yang, Reprogrammable Humidity-Driven Liquid Crystalline Polymer Actuator Enabled by Dynamic Ionic Bonds, *ACS Appl. Mater. Interfaces*, 2022, **14**, 17869–17877.
 - 85 X. Lu, C. P. Ambulo, S. Wang, L. K. Rivera-Tarazona, H. Kim, K. Searles and T. H. Ware, 4D-Printing of Photo-switchable Actuators, *Angew. Chem., Int. Ed.*, 2021, **60**, 5536–5543.
 - 86 C. P. Ambulo, M. J. Ford, K. Searles, C. Majidi and T. H. Ware, 4D-Printable Liquid Metal–Liquid Crystal Elastomer Composites, *ACS Appl. Mater. Interfaces*, 2021, **13**, 12805–12813.
 - 87 J. A. H. P. Sol, L. G. Smits, A. P. H. J. Schenning and M. G. Debije, Direct Ink Writing of 4D Structural Colors, *Adv. Funct. Mater.*, 2022, **32**, 2201766.
 - 88 Z. Li, J. Wang, Y. Xu, M. Shen, C. Duan, L. Dai and Y. Ni, Green and sustainable cellulose-derived humidity sensors: A review, *Carbohydr. Polym.*, 2021, **270**, 118385.
 - 89 P. Zhu, H. Ou, Y. Kuang, L. Hao, J. Diao and G. Chen, Cellulose Nanofiber/Carbon Nanotube Dual Network-Enabled Humidity Sensor with High Sensitivity and Durability, *ACS Appl. Mater. Interfaces*, 2020, **12**, 33229–33238.
 - 90 A. Kafy, A. Akther, M. I. R. Shishir, H. C. Kim, Y. Yun and J. Kim, Cellulose nanocrystal/graphene oxide composite film as humidity sensor, *Sens. Actuators, A*, 2016, **247**, 221–226.
 - 91 Y. P. Zhang, V. P. Chodavarapu, A. G. Kirk and M. P. Andrews, Structured color humidity indicator from reversible pitch tuning in self-assembled nanocrystalline cellulose films, *Sens. Actuators, B*, 2013, **176**, 692–697.
 - 92 Y.-D. He, Z.-L. Zhang, J. Xue, X.-H. Wang, F. Song, X.-L. Wang, L.-L. Zhu and Y.-Z. Wang, Biomimetic Optical Cellulose Nanocrystal Films with Controllable Iridescent Color and Environmental Stimuli-Responsive Chromism, *ACS Appl. Mater. Interfaces*, 2018, **10**, 5805–5811.
 - 93 R. Duan, M. Lu, R. Tang, Y. Guo and D. Zhao, Structural Color Controllable Humidity Response Chiral Nematic Cellulose Nanocrystalline Film, *Biosensors*, 2022, **12**, 707.
 - 94 M. K. Khan, M. Giese, M. Yu, J. A. Kelly, W. Y. Hamad and M. J. MacLachlan, Flexible Mesoporous Photonic Resins with Tunable Chiral Nematic Structures, *Angew. Chem., Int. Ed.*, 2013, **52**, 8921–8924.
 - 95 T. Lu, H. Pan, J. Ma, Y. Li, S. W. Bokhari, X. Jiang, S. Zhu and D. Zhang, Cellulose Nanocrystals/Polyacrylamide Composites of High Sensitivity and Cycling Performance To Gauge Humidity, *ACS Appl. Mater. Interfaces*, 2017, **9**, 18231–18237.
 - 96 C. Sun, D. Zhu, H. Jia, K. Lei, Z. Zheng and X. Wang, Humidity and Heat Dual Response Cellulose Nanocrystals/Poly(*N*-Isopropylacrylamide) Composite Films with Cyclic Performance, *ACS Appl. Mater. Interfaces*, 2019, **11**, 39192–39200.
 - 97 C. Ohm, M. Brehmer and R. Zentel, Liquid Crystalline Elastomers as Actuators and Sensors, *Adv. Mater.*, 2010, **22**, 3366–3387.
 - 98 M. Moirangthem, R. Arts, M. Merckx and A. P. H. J. Schenning, An Optical Sensor Based on a Photonic Polymer Film to Detect Calcium in Serum, *Adv. Funct. Mater.*, 2016, **26**, 1154–1160.
 - 99 J. E. Stumpel, D. J. Broer and A. P. H. J. Schenning, Stimuli-responsive photonic polymer coatings, *Chem. Commun.*, 2014, **50**, 15839–15848.
 - 100 A. Saha, Y. Tanaka, Y. Han, C. M. W. Bastiaansen, D. J. Broer and R. P. Sijbesma, Irreversible visual sensing of humidity using a cholesteric liquid crystal, *Chem. Commun.*, 2012, **48**, 4579–4581.
 - 101 P. V. Shibaev, R. L. Sanford, D. Chiappetta and P. Rivera, Novel Color Changing pH Sensors Based on Cholesteric Polymers, *Mol. Cryst. Liq. Cryst.*, 2007, **479**, 161/[1199]–1167/[1205].
 - 102 P. V. Shibaev, D. Chiappetta, R. L. Sanford, P. Palffy-Muhoray, M. Moreira, W. Cao and M. M. Green, Color Changing Cholesteric Polymer Films Sensitive to Amino Acids, *Macromolecules*, 2006, **39**, 3986–3992.
 - 103 D. J. Mulder, A. P. H. J. Schenning and C. W. M. Bastiaansen, Chiral-nematic liquid crystals as one dimensional photonic materials in optical sensors, *J. Mater. Chem. C*, 2014, **2**, 6695–6705.
 - 104 D.-b Myung, S. Hussain and S.-Y. Park, Photonic calcium and humidity array sensor prepared with reactive cholesteric liquid crystal mesogens, *Sens. Actuators, B*, 2019, **298**, 126894.
 - 105 C.-K. Chang, C. M. W. Bastiaansen, D. J. Broer and H.-L. Kuo, Alcohol-Responsive, Hydrogen-Bonded, Cholesteric Liquid-Crystal Networks, *Adv. Funct. Mater.*, 2012, **22**, 2855–2859.
 - 106 J. E. Stumpel, C. Wouters, N. Herzer, J. Ziegler, D. J. Broer, C. W. M. Bastiaansen and A. P. H. J. Schenning, An Optical Sensor for Volatile Amines Based on an Inkjet-Printed, Hydrogen-Bonded, Cholesteric Liquid Crystalline Film, *Adv. Opt. Mater.*, 2014, **2**, 459–464.
 - 107 R. Lan, J. Sun, C. Shen, R. Huang, L. Zhang and H. Yang, Reversibly and Irreversibly Humidity-Responsive Motion of Liquid Crystalline Network Gated by SO₂ Gas, *Adv. Funct. Mater.*, 2019, **29**, 1900013.
 - 108 C. Shen, Z. Wang, R. Huang, J. Bao, Z. Li, L. Zhang, R. Lan and H. Yang, Humidity-Responsive Photonic Crystals with pH and SO₂ Gas Detection Ability Based on Cholesteric Liquid Crystalline Networks, *ACS Appl. Mater. Interfaces*, 2022, **14**, 16764–16771.
 - 109 W. Hu, L. Wang, M. Wang, T. Zhong, Q. Wang, L. Zhang, F. Chen, K. Li, Z. Miao, D. Yang and H. Yang, Ultrastable liquid crystalline blue phase from molecular synergistic self-assembly, *Nat. Commun.*, 2021, **12**, 1440.
 - 110 W. Hu, J. Sun, Q. Wang, L. Zhang, X. Yuan, F. Chen, K. Li, Z. Miao, D. Yang, H. Yu and H. Yang, Humidity-Responsive Blue Phase Liquid-Crystalline Film with Reconfigurable and Tailored Visual Signals, *Adv. Funct. Mater.*, 2020, **30**, 2004610.
 - 111 X. Shi, Z. Deng, P. Zhang, Y. Wang, G. Zhou and L. T. de Haan, Wearable Optical Sensing of Strain and Humidity: A

- Patterned Dual-Responsive Semi-Interpenetrating Network of a Cholesteric Main-Chain Polymer and a Poly(ampholyte), *Adv. Funct. Mater.*, 2021, **31**, 2104641.
- 112 M. del Pozo, C. Delaney, C. W. M. Bastiaansen, D. Diamond, A. P. H. J. Schenning and L. Florea, Direct Laser Writing of Four-Dimensional Structural Color Microactuators Using a Photonic Photoresist, *ACS Nano*, 2020, **14**, 9832–9839.
 - 113 Y. Foelen and A. P. H. J. Schenning, Optical Indicators based on Structural Colored Polymers, *Adv. Sci.*, 2022, **9**, 2200399.
 - 114 Y. Foelen, D. A. C. van der Heijden, M. del Pozo, J. Lub, C. W. M. Bastiaansen and A. P. H. J. Schenning, An Optical Steam Sterilization Sensor Based On a Dual-Responsive Supramolecular Cross-Linked Photonic Polymer, *ACS Appl. Mater. Interfaces*, 2020, **12**, 16896–16902.
 - 115 D. Liu, C. W. M. Bastiaansen, J. M. J. den Toonder and D. J. Broer, Light-Induced Formation of Dynamic and Permanent Surface Topologies in Chiral–Nematic Polymer Networks, *Macromolecules*, 2012, **45**, 8005–8012.
 - 116 D. Liu, L. Liu, P. R. Onck and D. J. Broer, Reverse switching of surface roughness in a self-organized polydomain liquid crystal coating, *Proc. Natl. Acad. Sci. U. S. A.*, 2015, **112**, 3880.
 - 117 W. Feng, D. J. Broer, L. Grebikova, C. Padberg, J. G. Vancso and D. Liu, Static and Dynamic Control of Fingerprint Landscapes of Liquid Crystal Network Coatings, *ACS Appl. Mater. Interfaces*, 2020, **12**, 5265–5273.
 - 118 J. E. Stumpel, D. J. Broer and A. P. H. J. Schenning, Water-responsive dual-coloured photonic polymer coatings based on cholesteric liquid crystals, *RSC Adv.*, 2015, **5**, 94650–94653.
 - 119 Y. Yang, X. Zhang, Y. Chen, X. Yang, J. Ma, J. Wang, L. Wang and W. Feng, Bioinspired Color-Changing Photonic Polymer Coatings Based on Three-Dimensional Blue Phase Liquid Crystal Networks, *ACS Appl. Mater. Interfaces*, 2021, **13**, 41102–41111.
 - 120 X. Zhang, Y. Xu, C. Valenzuela, X. Zhang, L. Wang, W. Feng and Q. Li, Liquid crystal-templated chiral nanomaterials: from chiral plasmonics to circularly polarized luminescence, *Light: Sci. Appl.*, 2022, **11**, 223.
 - 121 H. Yu, B. Zhao, J. Guo, K. Pan and J. Deng, Stimuli-responsive circularly polarized luminescent films with tunable emission, *J. Mater. Chem. C*, 2020, **8**, 1459–1465.
 - 122 R. Lan, J. Bao, Z. Li, Z. Wang, C. Song, C. Shen, R. Huang, J. Sun, Q. Wang, L. Zhang and H. Yang, Orthogonally Integrating Programmable Structural Color and Photo-Rewritable Fluorescence in Hydrazone Photoswitch-bonded Cholesteric Liquid Crystalline Network, *Angew. Chem., Int. Ed.*, 2022, **61**, e202213915.